Human Molecular Genetics, 2018, Vol. 27, No. 18 3189–3205

doi: 10.1093/hmg/ddy224
Advance Access Publication Date: 11 June 2018
Original Article

ORIGINAL ARTICLE

Parkin mediates the ubiquitination of VPS35 and modulates retromer-dependent endosomal sorting

Erin T. Williams[1,2], Liliane Glauser[3], Elpida Tsika[3,†], Haisong Jiang[4], Shariful Islam[2] and Darren J. Moore[2,*]

[1]Van Andel Institute Graduate School, [2]Center for Neurodegenerative Science, Van Andel Research Institute, Grand Rapids, MI 49503, USA, [3]Brain Mind Institute, Swiss Federal Institute of Technology (EPFL), 1015 Lausanne, Switzerland and [4]Institute for Cell Engineering and Department of Neurology, Johns Hopkins University School of Medicine, Baltimore, MD 21205, USA

*To whom correspondence should be addressed at: Center for Neurodegenerative Science, Van Andel Research Institute, 333 Bostwick Ave NE, Grand Rapids, MI 49503, USA. Tel: +1-616-234-5346; Email: darren.moore@vai.org

Abstract

Mutations in a number of genes cause familial forms of Parkinson's disease (PD), including mutations in the *vacuolar protein sorting 35 ortholog* (*VPS35*) and *parkin* genes. In this study, we identify a novel functional interaction between parkin and VPS35. We demonstrate that parkin interacts with and robustly ubiquitinates VPS35 in human neural cells. Familial parkin mutations are impaired in their ability to ubiquitinate VPS35. Parkin mediates the attachment of an atypical poly-ubiquitin chain to VPS35 with three lysine residues identified within the C-terminal region of VPS35 that are covalently modified by ubiquitin. Notably, parkin-mediated VPS35 ubiquitination does not promote the proteasomal degradation of VPS35. Furthermore, parkin does not influence the steady-state levels or turnover of VPS35 in neural cells and VPS35 levels are normal in the brains of parkin knockout mice. These data suggest that ubiquitination of VPS35 by parkin may instead serve a non-degradative cellular function potentially by regulating retromer-dependent sorting. Accordingly, we find that components of the retromer-associated WASH complex are markedly decreased in the brain of parkin knockout mice, suggesting that parkin may modulate WASH complex-dependent retromer sorting. Parkin gene silencing in primary cortical neurons selectively disrupts the vesicular sorting of the autophagy receptor ATG9A, a WASH-dependent retromer cargo. Parkin is not required for dopaminergic neurodegeneration induced by the expression of PD-linked D620N VPS35 in mice, consistent with VPS35 being located downstream of parkin function. Our data reveal a novel functional interaction of parkin with VPS35 that may be important for retromer-mediated endosomal sorting and PD.

Introduction

Parkinson's disease (PD) is the most common neurodegenerative movement disorder characterized by motor symptoms including tremor, rigidity, bradykinesia and postural instability (1,2). Motor symptoms primarily result from the loss of dopaminergic neurons in the substantia nigra pars compacta resulting in reduced striatal dopamine (1,2). Although the majority of PD cases are idiopathic, 5–10% of cases are hereditary. Mutations in at least thirteen genes are known to cause familial forms of PD, including autosomal recessive mutations in the *parkin (PARK2)* gene and autosomal dominant mutations in the *vacuolar protein sorting 35 ortholog* (*VPS35, PARK17*) gene (3–6).

[†]Present address: AC Immune SA, EPFL Innovation Park, 1015 Lausanne, Switzerland.
Received: March 29, 2018. **Revised:** May 27, 2018. **Accepted:** June 4, 2018

Numerous PD-linked mutations in *parkin* have been identified including deletions, truncations and point mutations that typically result in a loss-of-function of the parkin protein (3,7). The *PARK2* gene encodes the 465 amino acid parkin protein that functions as an E3 ubiquitin ligase and belongs to the RING-between-RING (RBR) family (8). Parkin normally maintains neuronal health by ubiquitinating its protein substrates which targets them for proteasomal degradation. Parkin-mediated substrate degradation is important for the selective removal of damaged mitochondria via mitophagy and also plays a distinct role in mitochondrial biogenesis and maintenance (7). Parkin can also ubiquitinate non-mitochondrial proteins and participate in signaling or trafficking pathways through both degradative and non-degradative mechanisms (7).

Recent genetic and functional studies have revealed a novel role for parkin in endosomal sorting pathways. Parkin genetically interacts with the retromer protein VPS35 in *Drosophila*. Flies lacking one copy of both the *parkin* and *VPS35* genes (but neither gene alone) exhibit decreased climbing ability, increased sensitivity to mitochondrial stressors and dopaminergic neuronal loss (9). These pathogenic phenotypes could be rescued by overexpression of VPS35 but not by parkin (9). A second study has identified a role for parkin-mediated ubiquitination in the endolysosomal pathway by modulating the activity of its substrate Rab7a, an accessory protein to the retromer that aids in membrane binding (10). VPS35 and parkin have also been implicated in the formation of mitochondrial-derived vesicles (MDVs), raising the possibility that these two proteins may functionally interact to modulate MDV formation (11,12). These studies support a potential interaction of the PD-linked genes parkin and VPS35 in a common cellular pathway.

In the present study, we identify a novel functional interaction between parkin and VPS35 where parkin mediates the non-degradative ubiquitination of VPS35. We demonstrate that parkin deficiency leads to reduced levels of the retromer-associated WASH complex and cargo in mouse brain and parkin can regulate WASH complex-dependent retromer cargo sorting. We provide additional evidence suggesting that VPS35 lies downstream of parkin function in mice, consistent with prior studies in *Drosophila*.

Results

Interaction of VPS35 and parkin

As emerging data suggests a role for parkin in the endolysosomal pathway, we first sought to explore the biochemical interaction of parkin with the retromer subunit VPS35 in mammalian cells. Human SH-SY5Y neural cells co-expressing V5-tagged VPS35 and FLAG-tagged parkin were subjected to immunoprecipitation (IP) with anti-FLAG antibody. We find that VPS35 interacts with parkin (Fig. 1A). To determine whether PD-linked familial mutations in VPS35 influence the interaction with parkin, we conducted co-IP assays of V5-tagged VPS35 variants using anti-V5 antibody. WT VPS35 as well as the pathogenic D620N and putative pathogenic P316S mutations, interact robustly and equivalently with FLAG-tagged parkin (Fig. 1B). We next assessed the effects of familial mutations in parkin by IP of FLAG-tagged parkin variants with anti-FLAG antibody. Familial PD-linked mutations in parkin (T240R, R256C, P437L, G328E and C431F) can interact with V5-tagged VPS35 equivalent to WT parkin (Fig. 1C). To determine the domains of parkin that are required for its interaction with VPS35, co-IP assays were conducted with cells expressing HA-tagged domain fragments of parkin. We find that V5-tagged VPS35 interacts with full-length parkin and with domains encompassing residues 88–465, 220–403 and 220–318 of parkin but not with parkin residues 304–465 and 385–465 (Fig. 1D), suggesting that the RING1 domain (residues 238–293) is sufficient for the interaction with VPS35. VPS35 plays a key role in the retromer complex where it comprises the core trimeric cargo-selective complex together with VPS26 and VPS29. To determine whether parkin selectively interacts with VPS35 versus other retromer subunits, we compared the interaction of FLAG-tagged parkin with V5-tagged VPS26, VPS29 or VPS35 in cells by co-IP. We demonstrate that parkin selectively interacts with VPS35 but not with VPS26 or VPS29 (Fig. 1E). Taken together, our data demonstrate a selective interaction of parkin with the retromer subunit VPS35 via the RING1 domain of parkin that is not altered by familial PD-linked mutations in either protein.

Parkin mediates the ubiquitination of VPS35

To explore the functional nature of the interaction of parkin with VPS35, we examined whether parkin could mediate the ubiquitination of VPS35. SH-SY5Y cells co-expressing combinations of HA-tagged ubiquitin, FLAG-tagged parkin and V5-tagged VPS35 variants were subjected to IP with anti-V5 antibody and analyzed by Western blotting. The overexpression of parkin robustly increases the levels of HA-tagged ubiquitin species ($\geq$100 kDa) in the VPS35 IPs compared to the absence of exogenous parkin and/or ubiquitin (Fig. 2A). In addition, we observe the formation of high molecular weight (HMW) species of VPS35 in the anti-V5 IPs, indicating the covalent attachment of ubiquitin to VPS35, which is markedly increased upon parkin overexpression (Fig. 2A). Familial mutants of VPS35 (P316S or D620N) are ubiquitinated by parkin to a similar extent as WT VPS35 in these assays (Fig. 2A). These assays also reveal evidence of VPS35 ubiquitination in the absence of parkin, albeit at lower levels than in the presence of parkin (Fig. 2A), suggesting ubiquitination of VPS35 by an endogenous E3 ubiquitin ligase in these cells. Previous studies have shown that parkin can regulate the endolysosomal pathway and retromer by ubiquitination of Rab7a (10). As such, we sought to compare the extent of parkin-mediated ubiquitination of VPS35 to that of Rab7a in these assays. Combinations of HA-tagged ubiquitin and FLAG-tagged parkin together with GFP-tagged VPS35 or GFP-HA-tagged Rab7a were co-expressed in SH-SY5Y cells and subjected to IP with anti-GFP antibody. In these assays, parkin mediates the robust ubiquitination of VPS35 compared to Rab7a, despite higher levels of total Rab7a relative to VPS35 (Supplementary Material, Fig. S1). These data demonstrate that VPS35 is a robust substrate of parkin-mediated ubiquitination and may play an important role in regulating retromer function.

We next asked whether familial PD-linked mutations in parkin influence VPS35 ubiquitination. Using similar *in vivo* ubiquitination assays with FLAG-tagged parkin variants, we demonstrate that familial mutations in parkin (T240R, R256C, C431F, P437L and G328E) are all impaired in their ability to ubiquitinate VPS35 relative to WT parkin (Fig. 2B), despite their similar ability to interact with VPS35 (Fig. 1C). This observation is consistent with the notion that familial missense mutations in parkin act via a loss-of-function mechanism (7). Although parkin interacts selectively with VPS35 within the retromer (Fig. 1E), we assessed whether parkin-mediated ubiquitination is also selective for VPS35. Following IP of V5-tagged VPS35, VPS26 or VPS29, we detect increased covalent ubiquitin

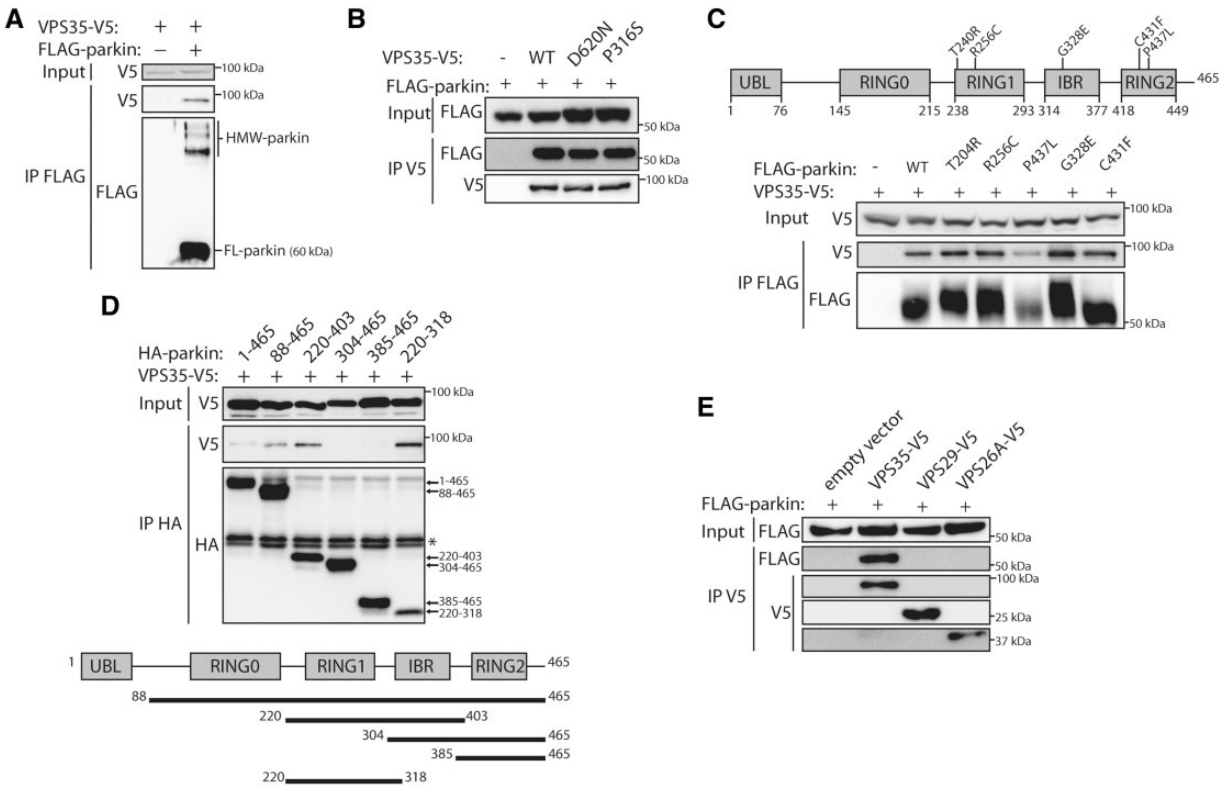

Figure 1. Interaction of VPS35 and parkin. (**A**) SH-SY5Y cells co-expressing FLAG-parkin and VPS35-V5 were subjected to immunoprecipitation (IP) with anti-FLAG antibody followed by Western blot analysis. Inputs and IPs were probed with anti-FLAG or anti-V5 antibodies. (HMW-parkin) denotes high molecular weight parkin that has undergone auto-ubiquitination. (**B**) SH-SY5Y cells co-expressing FLAG-parkin and V5-tagged VPS35 (WT, D620N or P316S) were subjected to IP with anti-V5 antibody followed by Western blot analysis. Inputs and IPs were probed with anti-V5 or anti-FLAG antibodies. (**C**) FLAG-tagged parkin familial mutants were co-transfected in SH-SY5Y cells with V5-VPS35 and subjected to IP with anti-FLAG antibody, and probed with anti-V5 and anti-FLAG antibodies. (**D**) HA-tagged parkin domains were co-transfected with VPS35-V5 in SH-SY5Y cells and subjected to IP with anti-HA antibody followed by Western blot analysis with anti-V5 and anti-HA antibodies. (*) denotes non-specific protein bands. (**E**) FLAG-parkin and V5-tagged retromer subunits were co-transfected in SH-SY5Y cells and subjected to IP with anti-V5 antibody followed by Western blot analysis with anti-V5 and anti-FLAG antibodies.

modification of VPS35 but not VPS26 or VPS29 in the presence of parkin and ubiquitin (Fig. 2C), confirming that parkin-mediated ubiquitination is selective for VPS35. Furthermore, we find no evidence for endogenous VPS26 or VPS29 ubiquitination in the absence of parkin in these assays (Fig. 2C), in contrast to VPS35, suggesting that ubiquitination of retromer subunits in general might be a specific property of VPS35. Since parkin selectively interacts with and ubiquitinates only VPS35, we assessed whether ubiquitinated VPS35 could be incorporated into the endogenous retromer complex. SH-SY5Y cells co-expressing combinations of HA-tagged ubiquitin, FLAG-tagged parkin and V5-tagged VPS35 were subjected to IP with an antibody to endogenous VPS26. We find increased HMW species containing HA-tagged ubiquitin (≥100 kDa) and covalently modified forms of VPS35 (in addition to full-length VPS35) in the VPS26 IPs in the presence of parkin (Fig. 2D), indicating that both ubiquitinated and non-ubiquitinated V5-tagged VPS35 can be incorporated into the endogenous retromer. Collectively, our data suggests that parkin mediates the robust and selective ubiquitination of VPS35 within the retromer.

Mitochondrial depolarization induces the vesicular dispersion of VPS35 but is not required for its ubiquitination by parkin

Parkin plays an important role in removing damaged mitochondria by mitophagy. Upon mitochondrial depolarization, parkin relocalizes from the cytoplasm to mitochondria upon its recruitment and activation by PINK1 where it ubiquitinates multiple proteins within the outer mitochondrial membrane to initiate mitophagy (13,14). Accordingly, we sought to determine whether mitochondrial damage could regulate the parkin-mediated ubiquitination of VPS35. To test this, SH-SY5Y cells co-expressing HA-tagged ubiquitin, FLAG-tagged parkin and V5-tagged VPS35 were treated with or without carbonyl cyanide m-chlorophenyl hydrazone (CCCP, 10 μM) to induce mitochondrial depolarization followed by IP with anti-V5 antibody to monitor VPS35 ubiquitination. Notably, parkin-mediated ubiquitination of VPS35 is modestly reduced upon CCCP treatment (Fig. 3A), consistent with reduced levels of parkin in the soluble fraction. The reduction in soluble parkin is most likely due to its movement to the insoluble fraction following mitochondrial recruitment. To determine whether CCCP treatment alters the turnover of VPS35, we monitored its steady-state levels in SH-SY5Y cells co-expressing HA-ubiquitin with or without FLAG-parkin. The levels of full-length and ubiquitinated VPS35 are not altered by CCCP (10 μM) whereas we can confirm that parkin shifts from the Triton-soluble to the Triton-insoluble fraction under these conditions (Fig. 3B). We next used immunofluorescent labeling to determine if CCCP treatment alters the levels of GFP-tagged VPS35 in SH-SY5Y cells. The levels of VPS35 measured using corrected total cell fluorescence (CTCF) are not significantly altered following 10 μM CCCP treatment (Fig. 3C

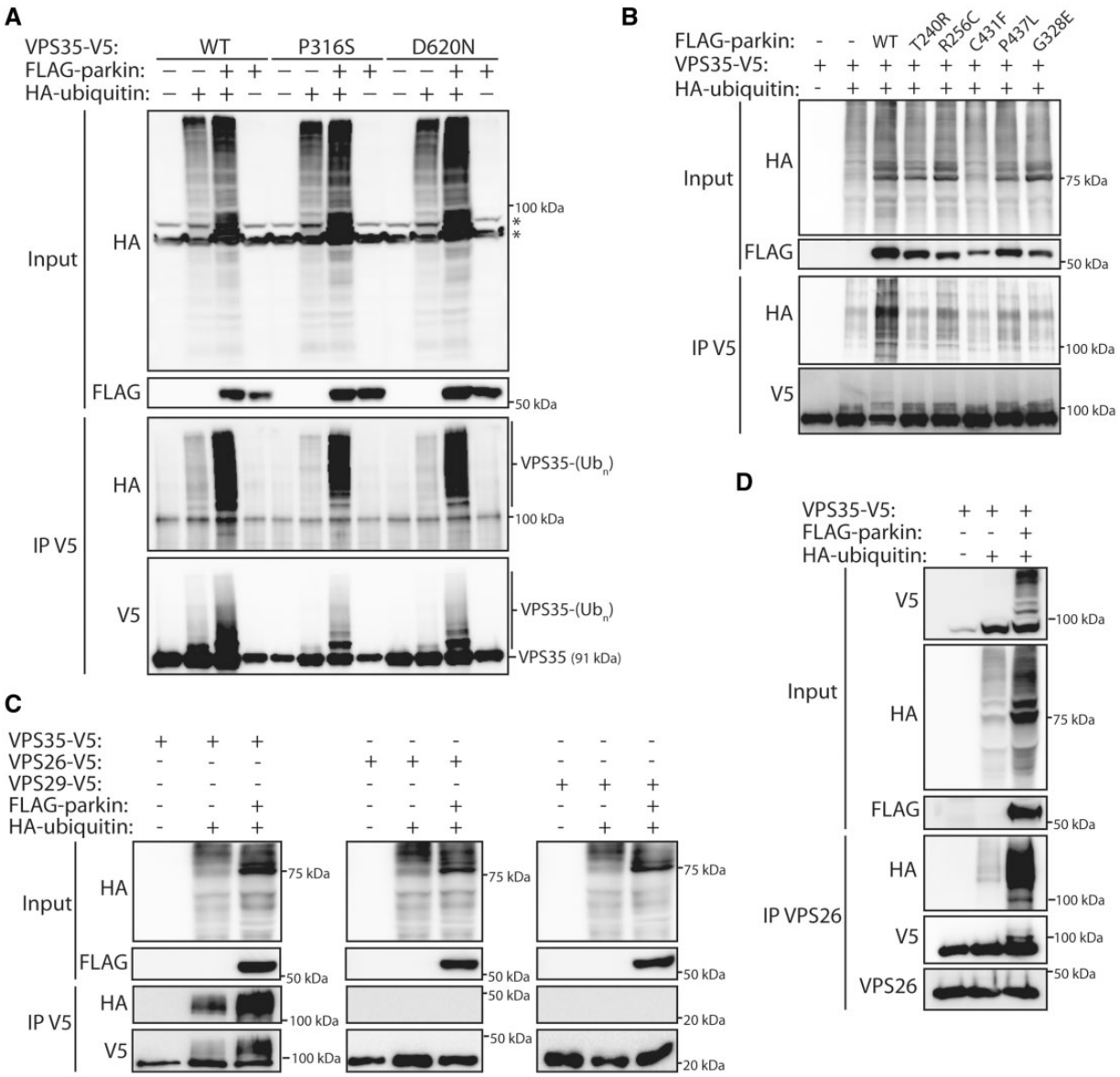

Figure 2. Parkin mediates the ubiquitination of VPS35. (**A**) SH-SY5Y cells co-expressing combinations of V5-tagged VPS35 variants, HA-ubiquitin and FLAG-parkin were subjected to IP with anti-V5 antibody followed by Western analysis. IPs and inputs were probed with anti-HA, anti-V5 and anti-FLAG antibodies. The ubiquitination of VPS35 variants is robustly increased in the presence of parkin. (**B**) FLAG-tagged parkin familial mutants were co-transfected with VPS35-V5 and HA-ubiquitin and subjected to IP with anti-V5 antibody followed by Western analysis with anti-HA, anti-V5 and anti-FLAG antibodies. (**C**) V5-tagged retromer subunits were co-transfected with FLAG-parkin and HA-ubiquitin and subjected to IP with anti-V5 antibody followed by Western analysis with anti-HA, anti-V5 and anti-FLAG antibodies. (**D**) Combinations of VPS35-V5, FLAG-parkin and HA-ubiquitin were co-transfected and subjected to IP with an antibody against endogenous VPS26. Western blots were probed with anti-HA, anti-V5, anti-FLAG and anti-VPS26 antibodies.

and D), consistent with Western data (Fig. 3B). To evaluate whether VPS35 is recruited to mitochondria under mitochondrial depolarization, similar to parkin, we conducted immunofluorescence co-localization analysis of GFP-tagged VPS35, mito-RFP and FLAG-tagged parkin treated with or without 10 μM CCCP (Fig. 3C). As expected, we demonstrate that parkin translocates to mitochondria under CCCP treatment, as revealed by the increased co-localization of FLAG-parkin and the mitochondrial marker, mito-RFP (Fig. 3E). Additionally, we show that the co-localization of VPS35 with mito-RFP or FLAG-parkin is significantly reduced by CCCP treatment, indicating that VPS35 does not translocate to mitochondria upon their depolarization (Fig. 3E). Under normal conditions, VPS35 co-localizes with both cytosolic parkin and mitochondria, suggesting that VPS35 may play a role in both locations (Fig. 3C and E).

Interestingly, we notice that the vesicular localization of VPS35 becomes highly dispersed throughout the cytoplasm upon CCCP treatment (Fig. 3C). To understand whether mitochondrial damage alters the endosomal localization of VPS35 or results in reorganization of the endosomal network, SH-SY5Y cells co-expressing V5-tagged VPS35 together with the endosomal markers, RFP-tagged Rab5 (early endosomes) and GFP-tagged Rab7 (late endosomes), were treated with or without 10 μM CCCP. Upon CCCP treatment, VPS35 as well as Rab5 and Rab7 compartments reveal a dispersed vesicular localization (Fig. 4A). VPS35 co-localizes normally with Rab5 and Rab7 upon

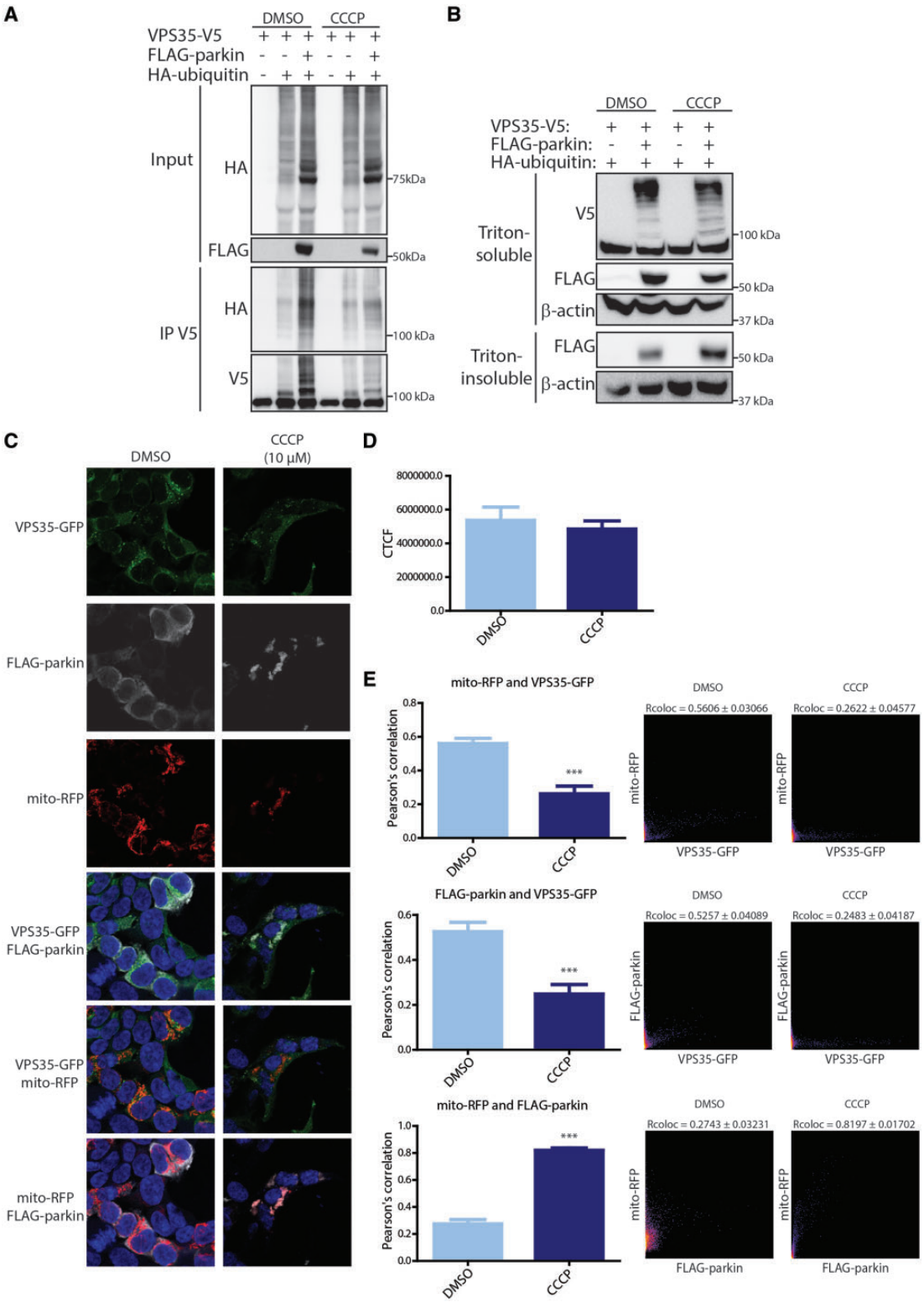

Figure 3. Mitochondrial depolarization induces VPS35 vesicular dispersal but is not required for its parkin-mediated ubiquitination. (**A**) SH-SY5Y cells co-expressing combinations of VPS35-V5, HA-ubiquitin and FLAG-parkin were treated with DMSO or CCCP (10 μM) for 2 h before harvesting. Lysates were subjected to IP with anti-V5 antibody followed by Western blot analysis with anti-V5, anti-HA and anti-FLAG antibodies. (**B**) Western blot analysis of 1% Triton-soluble and Triton-insoluble (RIPA-soluble) fractions from SH-SY5Y cells co-expressing combinations of VPS35-V5, HA-ubiquitin and FLAG-parkin following treatment with DMSO or CCCP (10 μM) for 2 h. The steady-state levels and solubility of V5-VPS35 and FLAG-parkin are shown relative to β-actin levels. (**C**) Representative confocal microscopic images of SH-SY5Y cells co-expressing VPS35-GFP, mito-RFP and FLAG-parkin treated with DMSO or CCCP (10 μM, 2 h). Nuclei are labeled with DAPI. (**D**) Bar graph showing CTCF values (mean ± SEM, $n \geq 18$ cells) of VPS35-GFP fluorescence levels in DMSO- or CCCP-treated cells. (**E**) Bar graphs indicating Pearson's correlation coefficients (Rcoloc; mean ± SEM, $n = 12$ cells/group) for co-localization of each protein pair in (**C**) as indicated. Data were analyzed by unpaired, two-tailed Student's *t*-test (***$P < 0.001$). Cytofluorograms and correlation coefficients (Rcoloc, mean ± SEM, $n = 12$ cells) indicate the degree of co-localization between fluorescent signals.

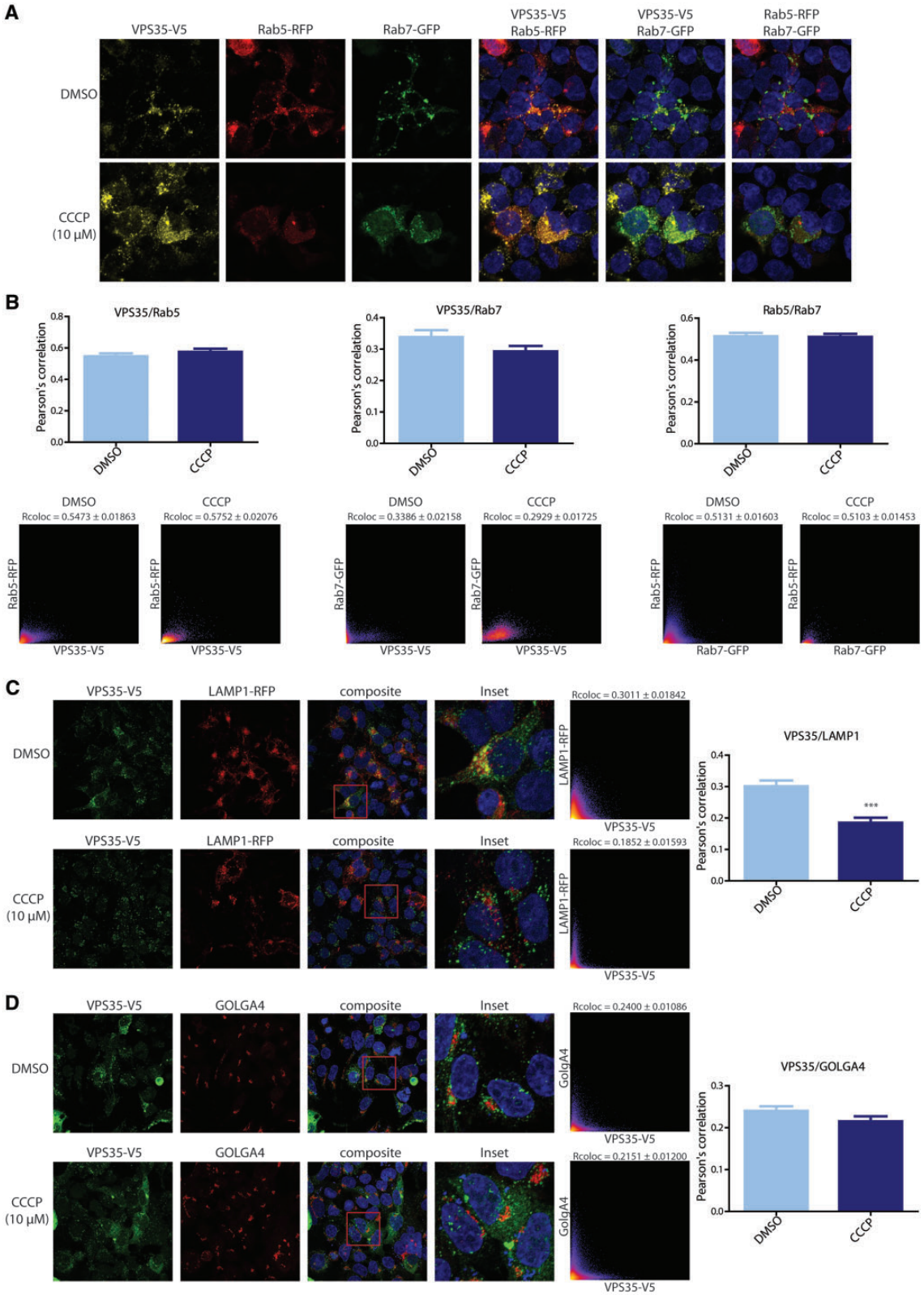

Figure 4. Mitochondrial depolarization induces the vesicular dispersal of VPS35 and endosomal markers. (A) Representative confocal immunofluorescent images of SH-SY5Y cells co-expressing VPS35-V5 (pseudo-colored yellow), Rab5-RFP (red) and Rab7-GFP (green) treated with CCCP (10 μM) or DMSO. Nuclei are labeled with DAPI. Overlays are shown for pairwise fluorescent channels, as indicated. (B) Graphs indicating Pearson's correlation coefficients (mean ± SEM, $n \geq 46$ cells/group) for co-localization of pairwise fluorescent signals in CCCP- and DMSO-treated cells. Cytofluorograms and correlation coefficients (Rcoloc, mean ± SEM, $n \geq 46$ cells) show the degree at which fluorescent signals co-localize. (C) Representative confocal immunofluorescent images of SH-SY5Y cells co-expressing VPS35-V5 (green) and LAMP1-RFP (red) treated with CCCP (10 μM) or DMSO. Graph and cytofluorograms indicate Pearson's correlation coefficients (mean ± SEM, $n = 54$ cells/group) for co-localization of VPS35 and LAMP1 signals in CCCP- and DMSO-treated cells. (D) Representative confocal immunofluorescent images of SH-SY5Y cells expressing VPS35-V5 (green) and endogenous GOLGA4 (red) treated with CCCP (10 μM) or DMSO. Graph and cytofluorograms indicate Pearson's correlation coefficients (mean ± SEM, $n = 60$ cells/group) for co-localization of VPS35 and GOLGA4 signals in CCCP- and DMSO-treated cells. Data were analyzed by unpaired, two-tailed Student's *t*-test (***$P < 0.001$), as indicated.

CCCP treatment, and the co-localization of Rab5 with Rab7 is also not altered (Fig. 4B). These data suggest that the vesicular dispersal of VPS35 following mitochondrial depolarization in cells is due to the reorganization of endosomal compartments. We similarly evaluated the effects of CCCP treatment on the co-localization of V5-tagged VPS35 with RFP-tagged LAMP1 (lysosomes) and endogenous GOLGA4 (*trans*-Golgi network, TGN), since the retromer is known to distribute to both compartments. Upon CCCP treatment, VPS35 co-localizes normally with GOLGA4 (Fig. 4D) but reveals a significantly reduced co-localization with LAMP1 (Fig. 4C). Whereas Rab5 and Rab7-positive vesicles are dispersed by CCCP treatment (Fig. 4A), the distribution of LAMP1-positive lysosomes and the TGN appear normal under these conditions (Fig. 4C and D). These data suggest that the reorganization of endosomal compartments by mitochondrial depolarization potentially reduces the sorting of VPS35 to lysosomes.

To understand whether the effects of mitochondrial depolarization are specific to VPS35 or generally influence the retromer complex, we conducted similar experiments with V5-tagged VPS29 in SH-SY5Y cells. Upon treatment with CCCP (10 μM), the vesicular localization of VPS29 becomes highly dispersed yet it co-localizes normally with Rab5 and Rab7 compartments (Supplementary Material, Fig. S2A and B). CCCP treatment similarly disperses the vesicular localization of endogenous VPS26 but does not alter its endosomal localization (Supplementary Material, Fig. S2C and D). We also demonstrate that CCCP treatment has minimal effects on the co-localization of endogenous VPS35 with VPS26 in SH-SY5Y cells but consistently induces the vesicular dispersal of both retromer subunits (Supplementary Material, Fig. S3). These data indicate that mitochondrial depolarization induces the vesicular dispersal of the retromer complex due to a reorganization of endosomal compartments. Together, our data demonstrate that mitochondrial depolarization is not required for the parkin-mediated ubiquitination of VPS35, does not affect VPS35 turnover, but does lead to the vesicular dispersal of VPS35 and the retromer complex along with endosomal compartments.

Parkin mediates the atypical poly-ubiquitination of VPS35

Parkin can mediate the attachment of several different types of ubiquitin linkage to its substrates, including poly-ubiquitin chains commonly linked via Lys48 or Lys63 residues, atypical poly-ubiquitin chains linked via Lys6 and Lys11, and mono-ubiquitination (8,15). To determine the nature of covalent ubiquitin attachment to VPS35 mediated by parkin, we employed a HA-tagged ubiquitin variant harboring a K48R mutation that can form any poly-ubiquitin linkage except Lys48-linked chains for *in vivo* ubiquitination assays with VPS35. We demonstrate that VPS35 ubiquitination mediated by parkin occurs equivalently with HA-tagged WT or K48R ubiquitin, suggesting that poly-ubiquitin chain attachment is not K48-linked, a chain linkage that normally targets substrates for proteasomal degradation (Fig. 5A). To provide further evidence of poly-ubiquitin chain attachment to VPS35 versus multiple mono-ubiquitination, we used an antibody (clone FK1) that specifically detects poly-ubiquitinated but not mono-ubiquitinated protein conjugates. Using *in vivo* ubiquitination assays, we detect the increased attachment of poly-ubiquitin chains (FK1-positive smear ≥100 kDa) to VPS35 IPs in the presence of parkin and ubiquitin (Fig. 5B), consistent with the increased smear containing HA-tagged ubiquitin that occurs at ≥100 kDa. The HMW nature of the ubiquitin-positive smear attached to VPS35 in addition to the FK1-positive signal strongly supports the poly-ubiquitination of VPS35 by parkin (Figs 2A–D and 5A and B).

Next, we attempted to determine the internal lysine residue(s) within VPS35 that are initially ubiquitinated by parkin. SH-SY5Y cells co-expressing V5-tagged VPS35 and HA-tagged ubiquitin in the presence or absence of FLAG-tagged parkin were subjected to IP with anti-V5 antibody to enrich for VPS35, resolved by SDS-PAGE and detected by staining with Coomassie colloidal blue (Fig. 5C). The gel region immediately above full-length VPS35 was excised to capture the first VPS35-ubiquitin species, digested with trypsin and analyzed by LC-MS/MS (Fig. 5C). The LC-MS/MS analysis achieved ∼50% sequence coverage of VPS35 and captured ∼70% of all lysine residues. Peptides containing a ubiquitinated lysine residue produce a di-glycine adduct after trypsin digestion that results in an increase in mass-to-charge ratio (16). Mass spectrometry identifies six lysine residues clustered within the C-terminal region of VPS35 that are modified by ubiquitin (i.e. di-glycine), three of which are specifically dependent on parkin overexpression (K515, K555 and K701) whereas three are endogenous (K659, K662 and K694) (Fig. 5C). Two of these lysine residues (K659 and K694) are known sites of ubiquitination according to PhosphoSitePlus. Importantly, three of the ubiquitinated lysine residues (K555, K662 and K701) are directly adjacent to another lysine (K556, K663 and K702) within the peptide identified by mass spectrometry, making a definitive assignment uncertain. Figure 5D provides an example of an annotated MS/MS spectra for a ubiquitinated peptide in the presence of parkin with the modified lysine indicated by gl*.

Interestingly, all identified lysine residues cluster within the C-terminal region of VPS35 (residues 515–701), a region known to mediate key interactions with VPS29 and the WASH complex (17–19). The PD-linked D620N mutation in this region impairs the interaction of VPS35 with FAM21, a component of the pentameric WASH complex (20, 21). Our data raise the possibility that ubiquitination within this region could regulate VPS35 interactions. To evaluate whether ubiquitination at these sites influences retromer assembly and interaction with the WASH complex, we individually mutated the six identified (and three adjacent) lysine residues to arginine in VPS35 to block endogenous ubiquitination. For co-IP assays, HEK-293T cells expressing V5-tagged VPS35 variants were subjected to IP with anti-V5 antibody. VPS35 harboring nine distinct K→R mutations interact equivalently with endogenous VPS26, VPS29 and WASH1, a core component of the WASH complex, relative to WT VPS35 (Fig. 5E). These data suggest that endogenous ubiquitination at these lysine residues does not regulate retromer assembly or recruitment of the WASH complex. Since ubiquitination modifies only a small proportion of total VPS35 in our assays, it is not possible to determine whether VPS35-ubiquitin conjugates directly influence interactions within the retromer. We next assessed whether K→R mutations in VPS35 block parkin-mediated ubiquitination. *In vivo* ubiquitination assays conducted in SH-SY5Y cells co-expressing V5-tagged VPS35 variants, FLAG-tagged parkin and HA-tagged ubiquitin were subjected to IP with anti-V5 antibody to monitor VPS35 ubiquitination. Unexpectedly, mutation of parkin-specific ubiquitination sites (K515R, K555R or K701R) or the adjacent lysine residues (K556R or K702R) does not appreciably diminish VPS35 ubiquitination (Fig. 5F), suggesting that parkin may ubiquitinate VPS35 simultaneously at multiple sites. We also generated a triple K→R mutant of VPS35 (K515R/K555R/K701R) lacking the three

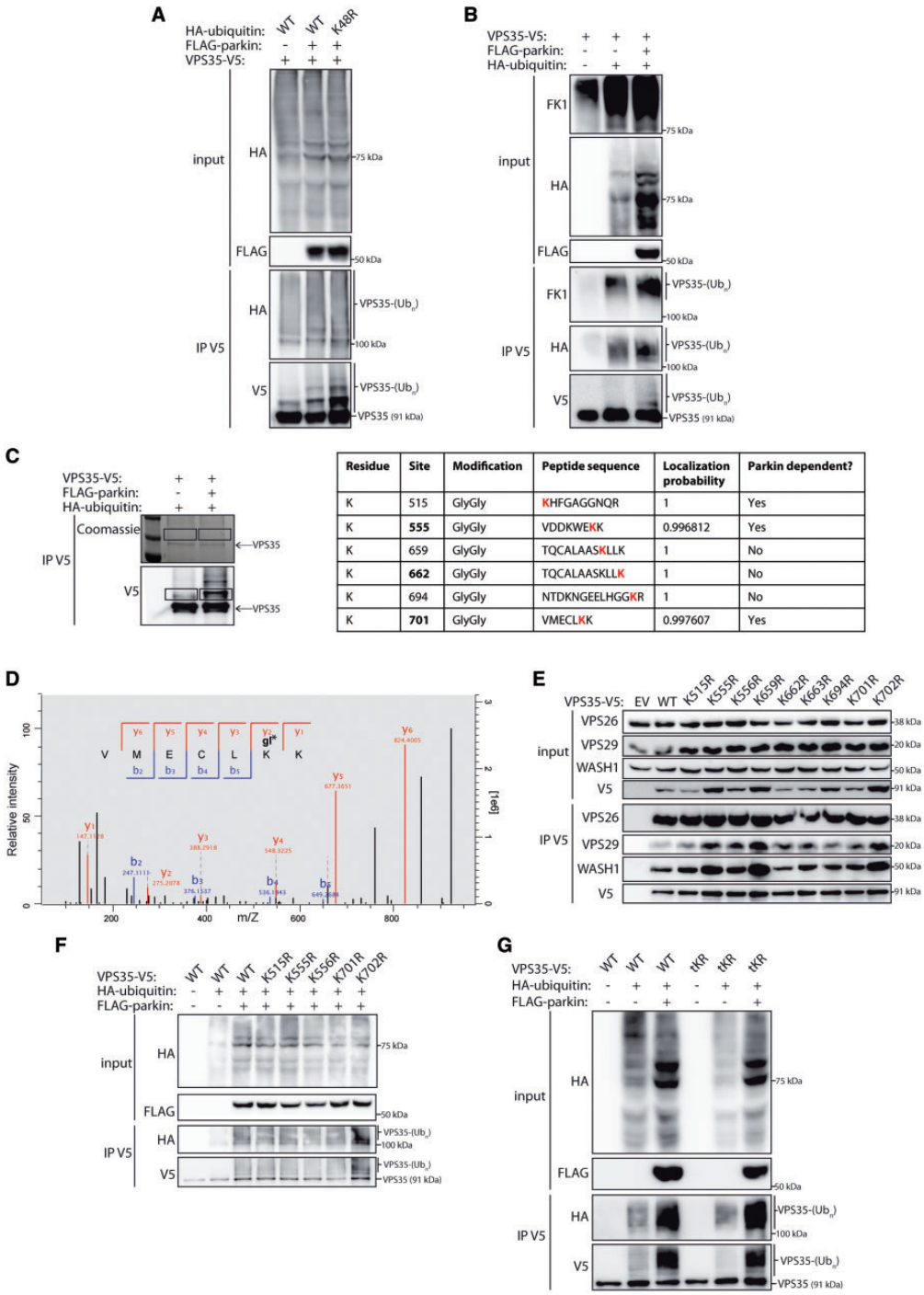

Residue	Site	Modification	Peptide sequence	Localization probability	Parkin dependent?
K	515	GlyGly	KHFGAGGNQR	1	Yes
K	**555**	GlyGly	VDDKWEKK	0.996812	Yes
K	659	GlyGly	TQCALAASKLLK	1	No
K	**662**	GlyGly	TQCALAASKLLK	1	No
K	694	GlyGly	NTDKNGEELHGGKR	1	No
K	**701**	GlyGly	VMECLKK	0.997607	Yes

Figure 5. Parkin mediates the atypical poly-ubiquitination of VPS35. (**A**) SH-SY5Y cells co-expressing combinations of VPS35-V5, HA-ubiquitin (WT or K48R) and FLAG-parkin were subjected to IP with anti-V5 antibody followed by probing of IPs and inputs with anti-HA, anti-V5 and anti-FLAG antibodies. Parkin-mediated ubiquitination of VPS35 is not altered using K48R ubiquitin. (**B**) SH-SY5Y cells co-expressing combinations of VPS35-V5, HA-ubiquitin and FLAG-parkin were subjected to IP with anti-V5 antibody and IPs and inputs were probed with FK1 (poly-ubiquitin-specific), anti-HA, anti-V5 and anti-FLAG antibodies. Parkin-mediated ubiquitination of VPS35 produces a strong FK1 signal similar to anti-HA antibody. (**C**) SH-SY5Y cells co-expressing combinations of VPS35-V5, HA-ubiquitin and FLAG-parkin were subjected to IP with anti-V5 antibody, and IPs were resolved by SDS-PAGE and gels subjected to staining with Coomassie blue or Western blot analysis with anti-V5 antibody. The boxed region indicates the gel fragment analyzed by LC-MS/MS. The table indicates the lysine residues of VPS35 identified as ubiquitinated (GlyGly modification) by LC-MS/MS analysis, the peptide sequence identified (with lysine residues in bold), localization probability (A score), and whether the modification requires parkin overexpression. (**D**) Representative annotated MS/MS spectra for a ubiquitinated peptide of VPS35 (at K701) in the presence of parkin. The diglycine-modified lysine and its position in the peptide sequence are indicated by gl*. (**E**) HEK-293T cells expressing V5-tagged VPS35 variants containing individual lysine to arginine mutations were subjected to IP with anti-V5 antibody and IPs and inputs were probed with anti-V5, anti-VPS26, anti-VPS29 and anti-WASH1 antibodies. VPS35 K→R mutants do not alter retromer assembly (VPS26 and VPS29) or interaction with the WASH complex (WASH1). (**F**) SH-SY5Y cells co-expressing combinations of V5-tagged VPS35 K→R mutants, HA-ubiquitin and FLAG-parkin were subjected to IP with anti-V5 antibody and IPs and inputs were probed with anti-HA, anti-V5 and anti-FLAG antibodies. Individual K→R mutants do not disrupt parkin-mediated VPS35 ubiquitination. (**G**) SH-SY5Y cells co-expressing combinations of V5-tagged VPS35 with a triple K→R mutation (K515R/K555R/K701R; tKR), HA-ubiquitin and FLAG-parkin were subjected to IP with anti-V5 antibody and IPs and inputs were probed with anti-HA, anti-V5 and anti-FLAG antibodies. A triple lysine-to-arginine mutant representing all parkin-mediated ubiquitin attachment sites identified by LC-MS/MS does not diminish parkin-mediated ubiquitination.

parkin-specific lysine residues, however, this is not sufficient to inhibit the ubiquitination of VPS35 by parkin as compared to WT VPS35 (Fig. 5G). These data potentially suggest that parkin may ubiquitinate VPS35 at additional lysine residues not identified by LC-MS/MS analysis, and/or could indicate the multiple mono-ubiquitination of VPS35 at several different sites (a feature supported by the identification of three internal ubiquitin attachment sites in VPS35). Taken together, our data demonstrate that parkin mediates the ubiquitination of VPS35 on at least three distinct lysine residues consistent with multiple mono-ubiquitination and we find evidence for poly-ubiquitin chain attachment suggesting an atypical form of VPS35 ubiquitination.

Ubiquitination of VPS35 by parkin is not a signal for proteasomal degradation

To understand the consequences of VPS35 ubiquitination, we sought to determine whether parkin enhances VPS35 protein turnover via proteasomal degradation. Ubiquitination assays were conducted as described before in SH-SY5Y cells in the presence or absence of the proteasome inhibitor MG132. In the presence of MG132, parkin expression produces a modest increase in VPS35 ubiquitination (HA-ubiquitin signal) compared to the control treatment with DMSO (Fig. 6A). However, the apparent increased ubiquitination is due to higher levels of VPS35 in this IP fraction from MG132-treated cells (Fig. 6A). While this data suggests that a small proportion of non-ubiquitinated VPS35 is normally degraded by the proteasome, ubiquitinated VPS35 induced by parkin does not specifically accumulate following proteasome inhibition. Similar results are obtained with a second highly specific proteasomal inhibitor, *clasto*-lactacystin β-lactone (Fig. 6B). In the absence of parkin, MG132 consistently leads to a marked increase in full-length and ubiquitinated VPS35 to a greater extent than with parkin overexpression (Fig. 6A), potentially suggesting that parkin may interfere with VPS35 ubiquitination by an endogenous E3 ubiquitin ligase. Next, we evaluated whether parkin-mediated ubiquitination

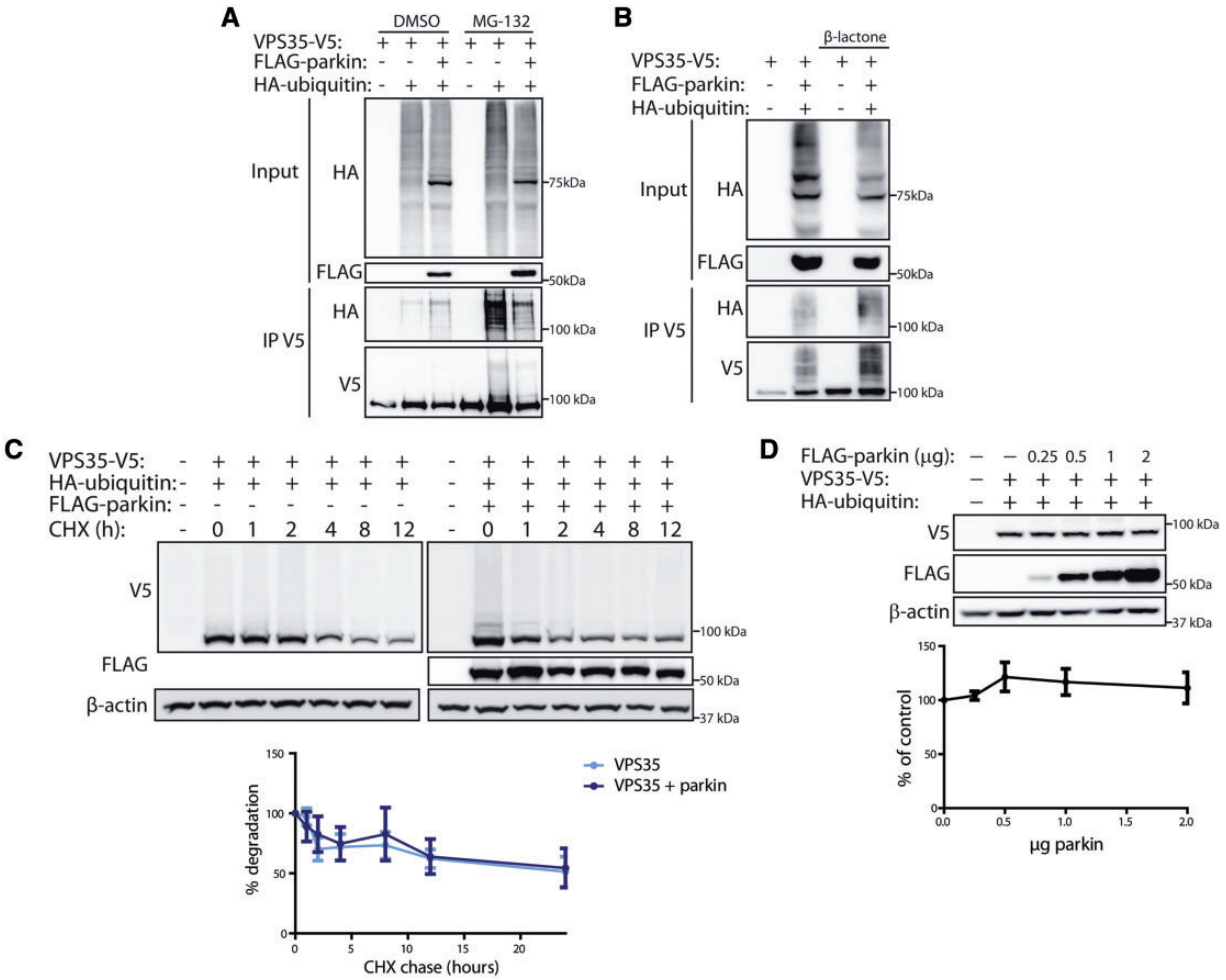

Figure 6. Parkin-mediated ubiquitination of VPS35 does not induce its degradation. (**A**) SH-SY5Y cells co-expressing combinations of VPS35-V5, FLAG-parkin and HA-ubiquitin were treated with the proteasome inhibitor MG132 (5 μM) or DMSO for 24 h and then subjected to IP with anti-V5 antibody and Western analysis. MG132 treatment does not robustly increase parkin-mediated VPS35 ubiquitination. (**B**) Similar experiment to (**A**) but with treatment with the proteasome inhibitor *clasto*-lactacystin β-lactone (10 μM) for 24 h. β-lactone treatment does not robustly increase parkin-mediated VPS35 ubiquitination. (**C**) SH-SY5Y cells co-expressing VPS35-V5 and HA-ubiquitin with or without FLAG-parkin were treated with cycloheximide (CHX, 200 μg/ml) and cells were harvested at 0, 1, 2, 4, 8 and 12 h post-treatment. Equivalent levels of triton-soluble fractions were probed with anti-V5, anti-FLAG or anti-actin antibodies to monitor the rate of VPS35 turnover. Graph indicates quantitation of VPS35 levels normalized to actin and expressed as a percent of time point 0 for each condition (mean ± SEM, $n = 5$). (**D**) Equivalent triton-soluble fractions from SH-SY5Y cells co-expressing VPS35-V5, HA-ubiquitin and increasing amounts of FLAG-parkin (0.25–2 μg plasmid DNA) were probed with anti-V5, anti-FLAG or anti-actin antibodies to monitor VPS35 steady-state levels. Graph indicates quantitation of VPS35 levels normalized to actin and expressed as a percent of VPS35 alone (mean ± SEM, $n = 4$).

alters the rate of VPS35 turnover. SH-SY5Y cells co-expressing V5-tagged VPS35 and HA-tagged ubiquitin with or without FLAG-tagged parkin were treated with the protein synthesis inhibitor cycloheximide (CHX) and VPS35 levels were monitored over 12 h. The presence of parkin in this assay has no effect on the rate of VPS35 turnover (Fig. 6C), further supporting the idea that parkin-mediated ubiquitination of VPS35 is non-degradative. Additionally, in SH-SY5Y cells expressing a constant amount of V5-tagged VPS35, progressively increasing the amount of FLAG-tagged parkin does not influence the steady-state levels of VPS35 (Fig. 6D). Together, our data suggest that parkin-mediated ubiquitination of VPS35 is not a signal for its proteasomal degradation and raises the possibility that VPS35 ubiquitination may instead serve to regulate retromer function.

Parkin deficiency reduces WASH complex and cargo levels in mouse brain

To further confirm the non-degradative nature of parkin-mediated VPS35 ubiquitination in cells, we extended our studies to mouse brain. Accordingly, the steady-state levels of endogenous VPS35 were examined in two different parkin knockout (KO) mouse models. First, VPS35 levels were measured in ventral midbrain extracts from adult homozygous conditional parkin KO mice (harboring a floxed exon 7) at 4 weeks following the intranigral delivery of a lentiviral vector expressing GFP-Cre (or lenti-GFP as a control) to delete parkin at post-natal stages in order to avoid any developmental compensation (22,23). We demonstrate that VPS35 levels are not altered in brain following the Cre-dependent deletion of parkin in conditional KO mice relative to control mice (cKO + GFP), whereas parkin levels are undetectable following Cre expression in KO mice (Fig. 7A). We also used germline parkin KO mice (harboring an exon 3 deletion) to further evaluate the levels of endogenous retromer subunits and cargo in the brain. The levels of retromer subunits VPS35, VPS26 and VPS29 remain unchanged in the ventral midbrain of parkin KO mice compared to WT mice (Fig. 7B and C), whereas VPS35 and VPS26 are modestly increased in the striatum of KO mice (Fig. 7D and E). We demonstrate that the WASH complex subunits WASH1 and FAM21 are significantly reduced in the ventral midbrain of parkin KO mice (Fig. 7B and C), whereas WASH1 and the WASH-dependent retromer cargo ATG9A are also reduced in the striatum of KO mice (Fig. 7D and E). Reduced WASH1 levels are also observed in substantia nigra dopaminergic neurons of parkin KO mice by confocal immunofluorescent microscopy (Fig. 7F) consistent with reduced levels in ventral midbrain extracts (Fig. 7B and C). Our data demonstrate that the absence of parkin in mice results in reduced levels of the WASH complex and WASH-dependent retromer cargo in the nigrostriatal dopaminergic pathway, potentially suggesting a normal role for parkin and VPS35 ubiquitination in stabilizing the retromer-associated WASH complex.

Parkin regulates sorting of WASH-dependent retromer cargo in neurons

As WASH complex subunits and WASH-dependent retromer cargo are reduced in brains of parkin KO mice, we next asked whether parkin could regulate retromer cargo sorting in neurons. Rat primary cortical neurons were infected with lentiviral vectors expressing short hairpin RNAs (shRNA) targeting parkin or a control shRNA. Infection of cortical neurons with increasing doses of two distinct parkin-directed shRNAs results in the dose-dependent knockdown of endogenous parkin protein (Fig. 8A). We selected the most efficient shRNA (#1) for parkin gene silencing in the subsequent experiments. Using confocal microscopy we demonstrate that the levels and subcellular localization of VPS35 are not altered by parkin gene silencing (Fig. 8B). Next, we examined the levels and subcellular localization of ATG9A and WASH1 in cortical neurons following parkin knockdown. While ATG9A levels remain unchanged in the absence of parkin in MAP2-positive cortical neurons, we do observe an altered localization of ATG9A characterized by its cytoplasmic dispersal in contrast to its normal punctate and perinuclear distribution (Fig. 8C). To further evaluate the dispersal of ATG9A following parkin silencing, we conducted confocal co-localization assays with markers of early endosomes (EEA1) and the *trans*-Golgi network (TGN46) in cortical neurons. We find a significant reduction of ATG9A co-localization with EEA1 upon parkin knockdown (Fig. 8D), but no change in its co-localization with TGN46 (Fig. 8E). WASH1 levels and co-localization with EEA1 are not altered following parkin gene silencing in cortical neurons (Supplementary Material, Fig. S4). We also examined a classical WASH-independent retromer cargo, sortilin (SORT1), to determine whether parkin selectively influences WASH-dependent cargo sorting. In contrast to ATG9A, sortilin levels and its co-localization with EEA1 or TGN46 in cortical neurons remain unchanged following parkin knockdown (Supplementary Material, Fig. S5). Taken together, our data suggest an important role for parkin in regulating retromer function in neurons, and reveal a specific effect on WASH-dependent retromer cargo sorting.

Parkin is not essential for neurodegeneration induced by PD-linked D620N VPS35 in mice

Prior studies in *Drosophila* models suggest a genetic interaction of parkin and VPS35, with VPS35 most likely located downstream of parkin activity (9). Our biochemical and cell biology data also tend to support such a hierarchical organization with parkin activity upstream of VPS35. To determine whether parkin plays a role in neurodegeneration induced by PD-linked D620N VPS35 *in vivo*, human D620N VPS35 was overexpressed in dopaminergic neurons of the substantia nigra of adult parkin KO mice or their WT littermates. Recombinant AAV2/6 vectors expressing V5-tagged human D620N VPS35, or an empty control virus (MCS), were stereotactically delivered to mice by a single unilateral intranigral injection. This AAV-VPS35 model was previously shown to induce a ~32% loss of nigral dopaminergic neurons in adult rats (24). At 12 weeks post-injection, we observe the robust and equivalent expression of D620N VPS35 in the ipsilateral substantia nigra of parkin KO and WT mice (Fig. 9A). To evaluate the extent of dopaminergic neurodegeneration, unbiased stereological methodology was used to count the number of tyrosine hydroxylase (TH)-positive and total Nissl-positive neurons in the ipsilateral nigra relative to the contralateral nigra. D620N VPS35 expression induces a robust loss of TH-positive dopaminergic neurons in WT mice (31.96% ± 8.813%), compared to an empty control virus, that is not significantly altered in parkin KO mice (31.99% ± 8.678%) (Fig. 9B). The loss of TH-positive neurons in WT and KO mice parallels the loss of Nissl-positive neurons, confirming neuronal loss rather than a loss of TH phenotype (Fig. 9C). These data suggest that parkin is not required for dopaminergic neurodegeneration induced by PD-linked D620N VPS35 in mice and confirms that parkin activity is most likely located upstream of VPS35 *in vivo*.

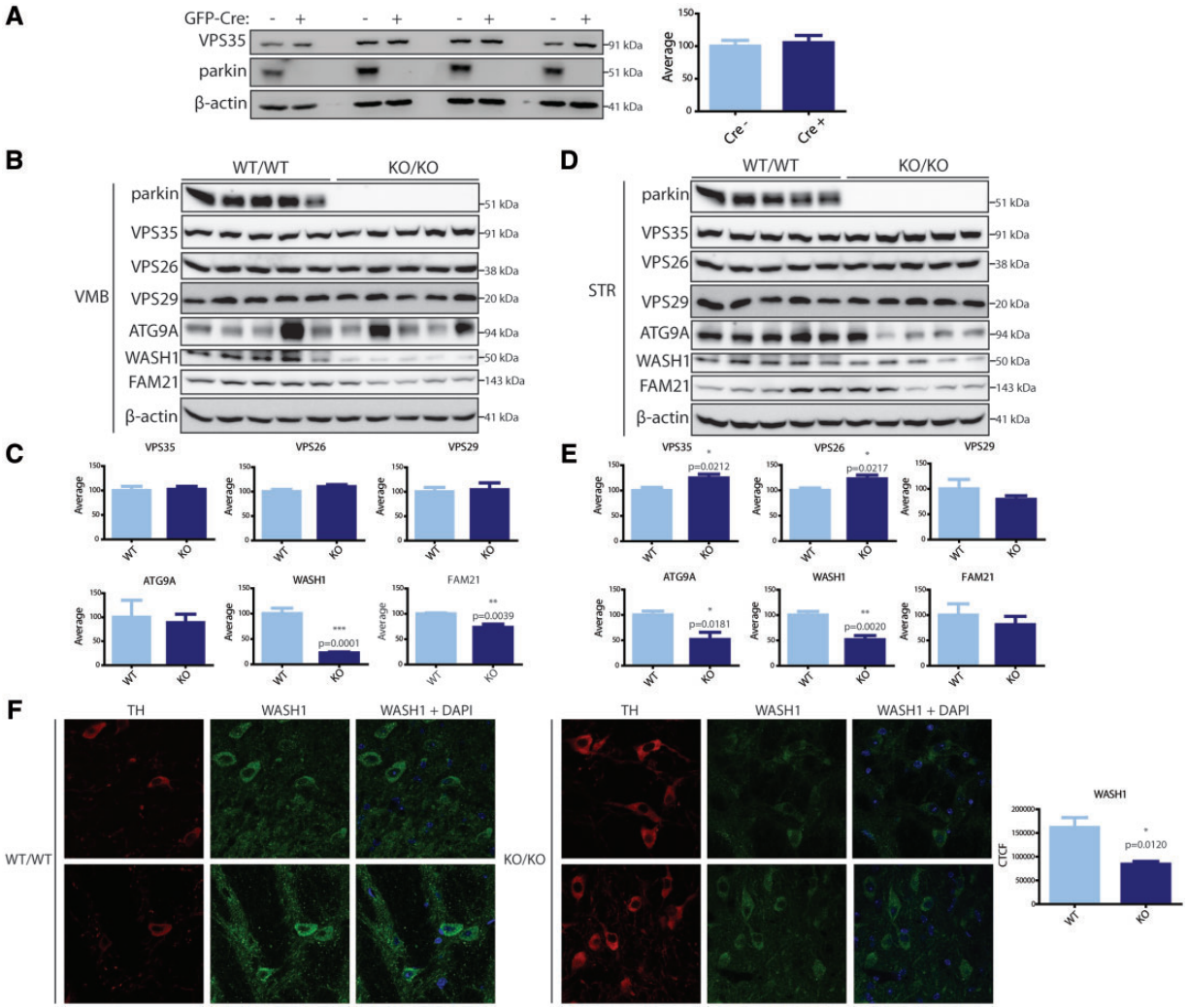

Figure 7. Parkin deficiency reduces WASH complex components and WASH-dependent retromer cargo in mouse brain. (**A**) Homozygous conditional parkin KO mice (*Parkin*$^{flox/flox}$, floxed exon 7) were subjected to intranigral injection of lentiviral vectors expressing GFP-Cre or GFP and at 4 weeks post-injection ventral midbrain extracts were analyzed by Western blotting to determine VPS35 levels. Parkin levels are undetectable following Cre expression. Graph indicates densitometric analysis of VPS35 levels normalized to actin expressed as a percent of the control group (mean ± SEM, $n = 4$ animals/group). (**B–D**) Triton-soluble fractions from ventral midbrain (**B**) or striatum (**D**) of adult germline parkin KO or WT littermate mice were subjected to Western blot analysis for retromer (VPS35, VPS26 or VPS29) and WASH complex (WASH1 or FAM21) subunits, WASH-dependent retromer cargo (ATG9A), parkin and β-actin. Graphs indicate densitometric analysis of each protein normalized to actin expressed as a percent of WT mice (mean ± SEM, $n = 5$ mice/group) in ventral midbrain (**C**) or striatum (**E**). Data were analyzed by unpaired, two-tailed Student's *t*-test ($^*P < 0.05$, $^{**}P < 0.01$, $^{***}P < 0.001$), as indicated. (**F**) Representative confocal images from substantia nigra tissue of germline parkin KO and WT mice indicating immunofluorescent co-labeling of endogenous WASH1 and dopaminergic neurons (TH). Graph indicates CTCF values for WASH1 in TH-positive dopaminergic neurons (mean ± SEM, $n \geq 8$ neurons/group) of WT or KO mice. Data were analyzed by unpaired, two-tailed Student's *t*-test ($^*P < 0.05$), as indicated.

However, it is not possible to confirm whether VPS35 is required downstream for parkin-dependent neurodegeneration since germline parkin KO mice do not typically exhibit neuronal loss, whereas heterozygous VPS35 deletion in mice is sufficient to induce progressive dopaminergic neurodegeneration.

Discussion

Here, we identify a novel functional interaction between two PD-linked proteins, the E3 ubiquitin ligase parkin and the retromer subunit VPS35. Parkin interacts selectively with VPS35 but not with other core members of the retromer complex, VPS26 or VPS29. The RING1 domain of parkin is sufficient for the interaction with VPS35 whereas familial PD-linked mutations in either protein have no effect. Parkin selectively mediates the robust ubiquitination of VPS35 and this modification is impaired by familial mutations in parkin. Mitochondrial depolarization is not required for parkin-mediated VPS35 ubiquitination but does induce the vesicular dispersal of VPS35 and the endosomal network. Parkin mediates the atypical ubiquitination of VPS35 with evidence for non-Lys48-linked poly-ubiquitin chain attachment upon at least three internal lysine residues clustering within its C-terminal region. Ubiquitination of VPS35 does not enhance its turnover via proteasomal degradation in cells, consistent with normal steady-state levels of VPS35 in brains from conditional and germline parkin knockout mice. Instead, the absence of parkin in knockout mice reduces the levels of WASH complex subunits (WASH1 and FAM21) and WASH-dependent retromer cargo (ATG9A) in the nigrostriatal dopaminergic pathway. We further find that parkin deficiency in a primary cortical neuronal model disrupts the endosomal localization of WASH-dependent (ATG9A) but not WASH-independent (sortilin) retromer cargo.

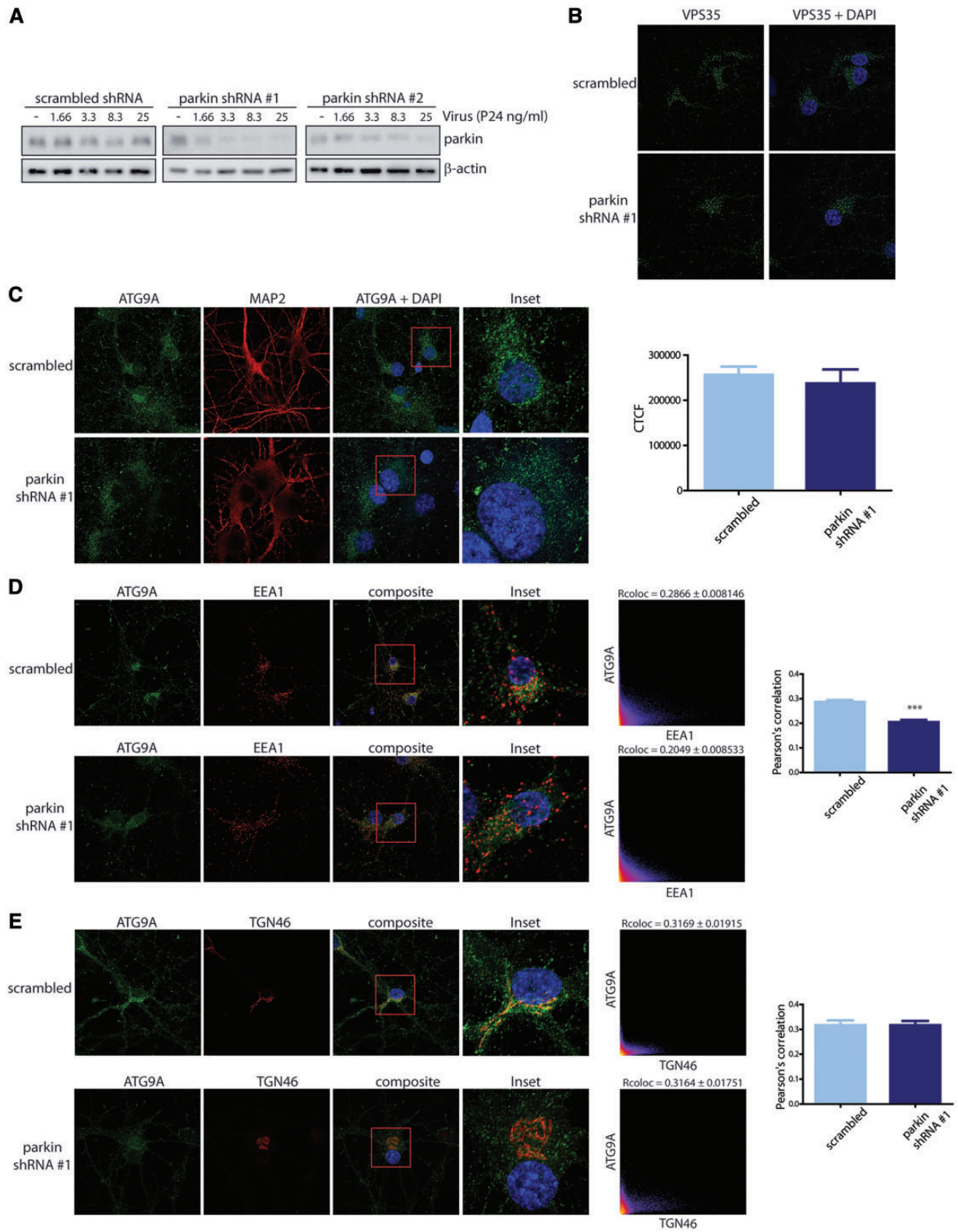

Figure 8. Parkin regulates sorting of WASH-dependent retromer cargo in neurons. (**A**) Western blot analysis of Triton-soluble extracts from rat primary cortical neurons infected with increasing titer of lentiviral vectors expressing parkin-directed (#1 and #2) or control shRNAs with anti-parkin or anti-actin antibodies. (**B**) Representative confocal immunofluorescent images of primary cortical neurons labeled with anti-VPS35 antibody. (**C**) Representative confocal images of cortical neurons co-labeled for ATG9A and the neuronal marker MAP2. Graph indicates CTCF values (mean ± SEM, $n \geq 16$ neurons/group) for the levels of ATG9A fluorescent signal in MAP2-positive neurons for both conditions. (**D and E**) Representative confocal immunofluorescent images of cortical neurons co-labeled for ATG9A and the early endosomal marker EEA1 (**D**) or the *trans*-Golgi marker TGN46 (**E**). Cytofluorograms and Pearson's correlation coefficients (Rcoloc, mean ± SEM, $n \geq 18$ neurons/group) indicate the degree of co-localization for the fluorescence signals of ATG9A with each subcellular marker. Data were analyzed by unpaired, two-tailed Student's t-test (***$P < 0.001$), as indicated.

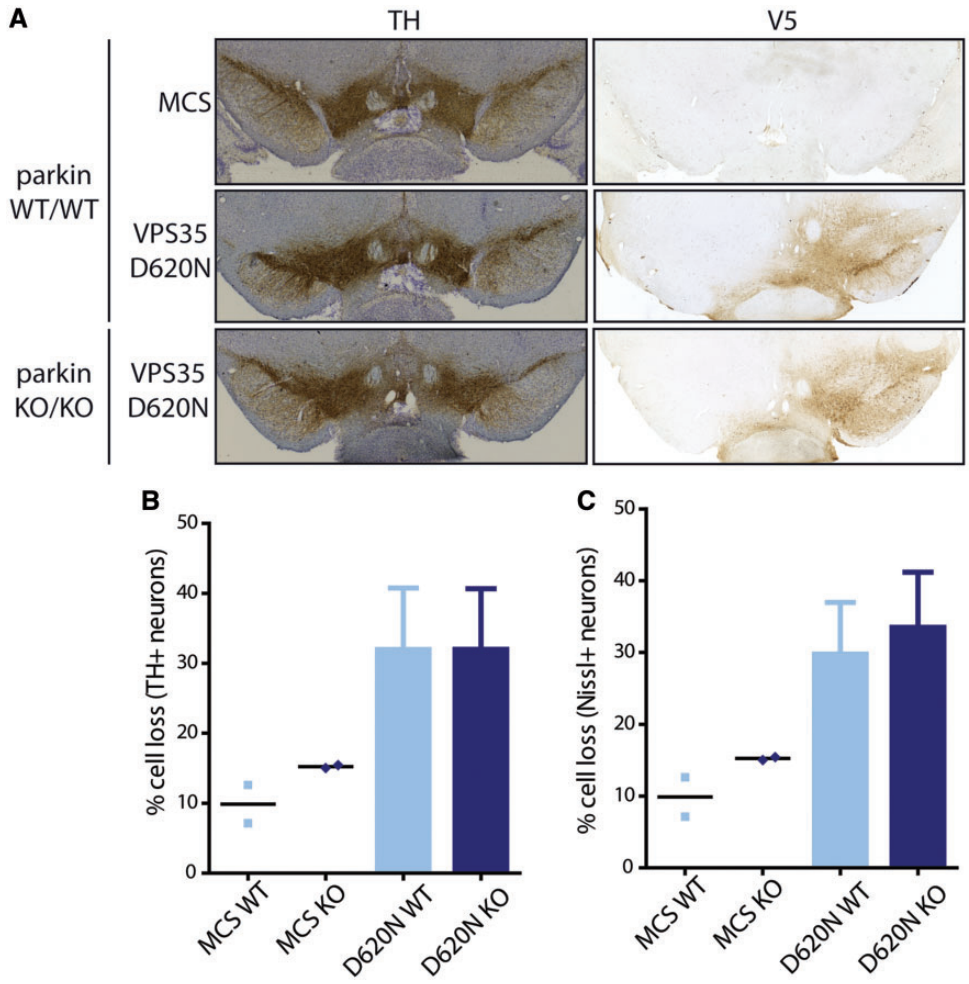

Figure 9. Parkin is not essential for dopaminergic neurodegeneration induced by human D620N VPS35 in mice. Adult germline parkin KO and WT littermate mice were subjected to unilateral intranigral injection of AAV2/6 vectors expressing V5-tagged human D620N VPS35, or control empty virus (MCS), and processed for immunohistochemistry after 12 weeks. (**A**) Representative photomicrographs of immunostaining for anti-TH (dopaminergic neurons) and anti-V5 (human VPS35) in the ipsilateral (injected, right) and contralateral (non-injected, left) substantia nigra of parkin KO and WT mice. (**B and C**) Unbiased stereological analysis of TH-positive dopaminergic neurons (**B**) or total Nissl-positive neurons (**C**) in the substantia nigra of parkin KO or WT mice, expressed as a percent of neuronal loss relative to the intact contralateral hemisphere. Graphs represent the percent neuronal loss (mean ± SEM, $n = 5–6$ animals/group) for the expression of D620N VPS35 in KO and WT mice. Data points indicate neuronal loss in two representative mice injected with AAV-MCS vector for each genotype (bar indicate mean loss). Data were analyzed by unpaired, two-tailed Student's *t*-test for D620N VPS35 groups only.

Finally, we demonstrate that parkin is not essential for nigral dopaminergic neurodegeneration in mice induced by human D620N VPS35 expression, supporting an upstream role for parkin in regulating VPS35. Collectively, our data reveal a novel functional interaction of parkin with VPS35 that may be important for regulating retromer-dependent cargo sorting in neurons.

The interaction of VPS35 with parkin and its ubiquitination is relatively selective within the retromer complex and does not extend to other subunits of the cargo-selective trimeric complex i.e. VPS26 or VPS29. Importantly, ubiquitinated VPS35 could be incorporated into the endogenous retromer suggesting that it is not likely to have a destabilizing effect on retromer assembly. Mass spectrometry analysis of covalent ubiquitin attachment sites identified three lysine residues in the C-terminal region of VPS35, a region that is important for binding to VPS29 and for recruiting the WASH complex via binding to FAM21. The PD-linked D620N mutation within this region has been shown to impair the interaction of VPS35 with the WASH complex (20,21). These data raise the distinct possibility that ubiquitination of VPS35 at these sites could serve as a signaling or stabilizing event for retromer assembly, WASH complex recruitment and/or cargo sorting. Such an effect would be consistent with the observation that poly-ubiquitination is non-Lys48-linked and does not target VPS35 for proteasomal degradation, indicating that ubiquitination most likely serves an alternative role other than simply regulating VPS35 turnover. However, null mutations at these three lysine residues (i.e. K515R, K555R or K701R) as well as adjacent sites (K556R or K702R) to block endogenous ubiquitination of VPS35 in cells failed to appreciably influence interactions with retromer or WASH complex subunits. Since ubiquitination of VPS35 modifies only a small proportion of the total protein (refer to Fig. 2A), the effects of these mutations on VPS35 binding to its partners is likely to be subtle and could be refractory to detection. Due to the low abundance of this modification in cells, it has not been possible to directly evaluate the impact of ubiquitin attachment to VPS35 on retromer complex assembly and WASH complex

recruitment. Instead, we provide indirect evidence that VPS35 ubiquitination potentially stabilizes these complex interactions by demonstrating that parkin deficiency leads to reduced levels of WASH complex subunits and cargo in the mouse brain and to abnormal WASH-dependent retromer cargo sorting in primary neurons. The stability of VPS35 itself is not regulated by parkin deficiency in primary neurons or mouse brain further suggesting that ubiquitination serves an alternative regulatory function. It is not yet clear whether the parkin-mediated ubiquitination of VPS35 at endogenous levels directly contributes to the normal sorting of WASH-dependent retromer cargo in neurons and brain since our data relied instead upon models of parkin deficiency. However, these data support a normal role for parkin in maintaining the stability and activity of the WASH complex in neurons.

In the absence of parkin-mediated ubiquitination of VPS35 in parkin knockout mice, the levels of WASH1, FAM21 and ATG9A are decreased in the brain. In the ventral midbrain (containing the substantia nigra) both WASH1 and FAM21 are reduced, whereas WASH1 and ATG9A are reduced in striatum. These data potentially suggest that the WASH-dependent retromer sorting of ATG9A to dopaminergic nerve terminals in the striatum is disrupted whereas normal levels are observed in the substantia nigra where dopaminergic neuronal soma are located. This sorting defect would be consistent with reduced WASH1 in both brain regions and specifically within nigral dopaminergic neurons. Further supporting such a mechanism, we provide evidence that ATG9A sorting is disrupted in primary cortical neurons by parkin gene silencing with reduced localization of ATG9A on early endosomes. In the absence of parkin it is possible that ATG9A remains within a specific compartment of the endolysosomal pathway, undergoes increased sorting to the plasma membrane or could be degraded by the lysosome. It remains unclear whether the impact of parkin on ATG9A levels and sorting in neurons is mediated directly by VPS35 ubiquitination and WASH complex recruitment, however, our biochemical data would strongly support such a mechanism. It will be important in future studies to determine if the sorting of other WASH-dependent retromer cargo, in addition to ATG9A, are dependent on parkin and are specifically regulated by VPS35 ubiquitination.

Previous studies support an interaction of parkin with VPS35 and the retromer. Parkin was reported to ubiquitinate Rab7a to regulate endosomal structure and function, and specifically altered the membrane association of VPS35 and levels of the retromer cargo, mannose 6-phosphate receptor (10). Rab7a plays a role in retromer function by recruiting and binding the core trimer (VPS26/29/35) at endosomal membranes (18). A comparison of Rab7 and VPS35 ubiquitination by parkin indicated that VPS35 is a more robust substrate in these cellular assays. These data suggest that parkin may play a general role in regulating endolysosomal sorting pathways via ubiquitination of key proteins such as VPS35 and Rab7 that could impact a number of endosomal cargo. A prior study in *Drosophila* models suggested a genetic interaction between VPS35 and parkin thereby suggesting that they might operate together in a common pathway (9). Flies with heterozygous null mutations in both genes developed a number of degenerative phenotypes that could be rescued by VPS35 overexpression but not by parkin (9). This observation suggests a common pathway with VPS35 located downstream of parkin. Our biochemical data are consistent with such a hierarchy with parkin mediating the downstream ubiquitination of VPS35. Furthermore, and similar to *Drosophila* studies (9), we find that parkin is dispensable for dopaminergic neurodegeneration induced by human D620N VPS35 expression, supporting an upstream role for parkin *in vivo*. These data also suggest that the endogenous ubiquitination of VPS35 by parkin in mouse brain (that is blocked in parkin KO mice) does not obviously contribute to its neurotoxic effects, most likely reflecting the small amount of total VPS35 that is modified by ubiquitin. Our future studies will aim to further delineate the parkin-VPS35 interaction *in vivo* by establishing whether parkin overexpression to oppositely *increase* VPS35 ubiquitination can mediate neuroprotection in PD-linked mutant VPS35 rodent models of PD. Collectively, our study together with prior work (9,10,25) provides compelling evidence for a novel functional interaction of parkin with VPS35 that may serve to regulate the sorting of WASH-dependent retromer cargo in neurons. Our findings suggest that parkin and VPS35 may function at least in part within a common pathway that will be important for understanding the pathophysiological mechanisms of both proteins in PD.

Materials and Methods

Animals

Timed pregnant female Sprague-Dawley outbred rats were obtained from Taconic Biosciences and P1 rats were used to prepare post-natal primary cortical neuronal cultures as previously described (26). Parkin knockout mice with a deletion of exon 3 (*Park2*^{tm1shn}, (27)) were obtained from The Jackson Laboratory (strain # 006582). Mice were maintained in a pathogen-free barrier facility and provided with food and water *ad libitum*, and exposed to a 12 h light/dark cycle. Animals were treated in strict accordance with the NIH Guild for the Care and Use of Laboratory Animals. All animal experiments were approved by the Van Andel Institute Institutional Animal Care and Use Committee (IACUC).

Expression plasmids and antibodies

A mammalian expression plasmid (pLenti6-V5/DEST) containing full-length human VPS35 with a C-terminal V5 tag was obtained from Addgene (#21691, (28)). D620N and P316S variants of VPS35 were generated as previously described (24). All lysine to arginine mutations (K515R, K555R, K556R, K659R, K662R, K663R, K694R, K701R and K702R) in VPS35 were created by site-directed mutagenesis (Agilent QuikChange II XL) and sequenced to confirm integrity. Human WT VPS35 cDNA was amplified by PCR and cloned in-frame into a pEGFP-N1 plasmid to create C-terminal GFP-tagged VPS35. Additionally, plasmids expressing Rab5-RFP (#14437; (29)), Rab7-GFP (#12605; (30)) and LAMP1-RFP (#1817) were obtained from Addgene. The pcB6-mito-RFP plasmid was kindly provided by Manuel Rojo (IBGC, Bordeaux, France). Short hairpin RNA (shRNA) sequences targeting rodent parkin (parkin-shRNA #1: TRCN0000041146; parkin-shRNA #2: TRCN0000041145) in lentiviral plasmid pLKO.1 were obtained from GE Life Sciences (Open Biosystems, Lafayette, CO). A pLKO.1 plasmid containing a control scrambled shRNA was obtained from Addgene (#1864; (31)). AAV2-PGK plasmids containing V5-tagged human D620N VPS35 or a control sequence (MCS) were previously described (24). FLAG-tagged full-length human parkin, HA-tagged human parkin domains and HA-tagged ubiquitin variants have been previously described (32). FLAG-tagged human parkin mutations (T240R, R256C, C431F, P437L and G328E) were introduced by subcloning partial ORF sequences from plasmids containing these myc-tagged parkin

variants (33) and verified by sequencing. To generate mammalian expression plasmids containing full-length human VPS26A and VPS29, cDNA (VPS26A: MHS6278–202806572; VPS29: MHS6278–202755971; Dharmacon) was PCR-amplified and first cloned into a pENTR/D-TOPO plasmid and recombined with a pcDNA3.2/V5-DEST plasmid using the Gateway cloning system to generate C-terminal V5-tagged VPS26A and VPS29 (Thermo Fisher).

The following primary antibodies were used: mouse anti-VPS35 (ab57632, Abcam), mouse anti-V5 and anti-V5-HRP (Invitrogen), mouse anti-FLAG and anti-FLAG-HRP (Sigma-Aldrich), rat anti-HA (clone 3F10, Roche), mouse anti-GFP (clone 7.1 and 13.1, Roche), rabbit anti-VPS26 (ab23892, Abcam), goat anti-VPS29 (ab10160, Abcam), mouse FK1 (Enzo Life Sciences), rabbit anti-WASH1 (Sigma-Aldrich), rabbit anti-ATG9A (ab108338, Abcam), mouse anti-parkin (Prk8 clone, Cell Signaling Technology), rabbit anti-Fam21A-D (S-13, Santa Cruz Biotechnology, Inc), mouse anti-MAP2 (Sigma-Aldrich), rabbit anti-Sortilin (ab16640, Abcam), mouse anti-EEA1 (clone 14, BD Biosciences), rabbit anti-tGolgin-1/GOLGA4 (kindly provided by Dr, Mickey Marks, University of Pennsylvania), mouse anti-TGN46 (clone 2F7.1, ab2809, Abcam), rabbit anti-TH (NB300–109, Novus Biologicals), mouse anti-TH (clone TH-2, Sigma-Aldrich) and mouse anti-actin (clone C4, Millipore). Secondary HRP-conjugated antibodies used for Western blotting were: goat anti-mouse IgG, light chain-specific (Jackson Immunoresearch), goat anti-rat IgG, light chain-specific (Jackson Immunoresearch), and mouse anti-rabbit IgG, light chain-specific (Jackson Immunoresearch). For confocal fluorescence analysis, the following secondary antibodies were used: AlexaFluor-488 or -647 goat anti-mouse IgG (H + L) and AlexaFluor-488 or -647 goat anti-rabbit IgG (H + L) (Thermo Fisher). For bright-field microscopy, the following biotinylated secondary antibodies were used: goat anti-mouse IgG and goat anti-rabbit IgG (Vector Labs).

Cell culture and transient transfection

Human SH-SY5Y neural cells and HEK-293T cells were maintained at 37°C with 5% CO_2 in Dulbecco's modified Eagle's media (DMEM) (Gibco) supplemented with 10% fetal bovine serum and penicillin/streptomycin. Transient transfection was performed with plasmid DNAs using XtremeGene HP DNA Transfection reagent (Roche) according to the manufacturer's instructions. Cells were harvested at 48 h post-transfection. Primary cortical neurons were maintained in 35 mm dishes on glass coverslips in Neurobasal media containing B27 supplement (2% w/v), L-glutamine (500 μM) and penicillin/streptomycin (100 U/ml). Neurons were infected with lentiviral vectors expressing shRNAs at DIV 3 and fixed at DIV 14 for immunocytochemistry. Where indicated, SH-SY5Y cells were treated with MG132 (5 μM; Enzo Life Sciences) or *clasto*-Lactacystin β-lactone (10 μM; Cayman Chemical) for 24 h prior to harvesting. To induce mitochondrial depolarization, SH-SY5Y cells were treated with 10 μM CCCP (Sigma) for 2 h prior to harvesting or fixation. For cycloheximide (CHX) chase assays in SH-SY5Y cells, CHX (200 μg/ml; Sigma) was added at 48 h post-transfection and cells were harvested at 0, 1, 2, 4, 8 or 12 h post-treatment. DMSO was used as a control treatment.

Co-immunoprecipitation and Western blotting

For co-immunoprecipitation (IP) assays, SH-SY5Y cells or HEK-239T cells were transiently transfected with the desired combination of plasmids in 10 cm dishes. At 48 h post-transfection, cells were harvested in 1 ml of lysis buffer (1× PBS, 1% Triton X-100, 1× Complete Mini protease inhibitor cocktail [Roche]). Cell lysates were allowed to rotate for 1 h at 4°C after which cell lysates were centrifuged at 15 000 rpm for 15 min at 4°C to collect the soluble fraction. Soluble fractions were mixed with Protein G-Dynabeads (Thermo Fisher) that had been pre-incubated with anti-V5 (1 μg), anti-FLAG (5 μg), anti-HA (5 μg) or anti-VPS26 (5 μg) antibody and incubated overnight at 4°C. All ubiquitination assays were stringently washed 5× with 1× PBS, 1% Triton X-100, 500 mM NaCl and 1× with 1× PBS. All other IP assays were washed as follows: 1× with 1× PBS, 1% Triton X-100 and 150 mM NaCl, 2× with 1× PBS, 1% Triton X-100 and 3× with 1× PBS. IPs were eluted by boiling at 95°C for 5 min in 50 μl of 2× Laemmli sample buffer. Inputs and IPs were subjected to SDS-PAGE, transferred to a nitrocellulose membranes, followed by Western blot analysis and imaging on a FujiFilm LAS-4000 Luminescent Image Analysis system. Where applicable, densitometry to quantify levels of proteins was performed using Image Studio Lite (LI-COR Biosciences).

Mass spectrometry

IP assays in SH-SY5Y cells were conducted as described above. 10 μl of each IP was used for Western blot analysis and the remaining 40 μl of IP was subjected to SDS-PAGE followed by staining with Coomassie colloidal blue (G-250, BIO-RAD). Gel fragments were excised above full-length VPS35 to capture VPS35-ubiquitin conjugates and analyzed by liquid chromatography tandem mass spectrometry (LC-MS/MS; MS Bioworks, Ann Arbor, MI). Briefly, gel fragments were digested with trypsin and analyzed by nano-LC-MS/MS with a Waters NanoAcquity HPLC system interfaced to a ThermoFisher Q Exactive. Peptides were loaded on a trapping column and eluted over a 75 μm analytical column at 350 nl/min with a 1 h reverse gradient; both columns were packed with Jupiter Proteo resin (Phenomenex). The mass spectrometer was operated in data-dependent mode, with Orbitrap operating at 60 000 FWHM and 17 500 FWHM for MS and MS/MS, respectively. The fifteen most abundant ions were selected for MS/MS. Data were searched using Mascot with GlyGly as a variable modification and parsed into Scaffold software for validation, filtering and to create a non-redundant list per sample. Data were filtered using a minimum protein value of 90%, a minimum peptide value of 50% (Prophet scores) and requiring at least two unique peptides per protein. Scaffold results were imported into Scaffold PTM in order to assign site localization probabilities using A-score (34). The minimum localization probability was set to 50%.

Immunocytochemistry

SH-SY5Y cells or primary cortical neurons seeded on coverslips in 35 mm dishes were fixed in 4% paraformaldehyde (PFA) and processed for immunocytochemistry analysis as previously described (26). Briefly, following fixation, coverslips were incubated with primary antibodies overnight at 4°C, followed by incubation with AlexaFluor-conjugated secondary antibodies at room temperature for 2 h. Coverslips were mounted onto glass slides using Prolong Diamond Antifade Mountant with DAPI (Thermo Fisher). Fluorescent images were acquired in x, y and z planes using a Nikon A1plus-RSi Laser Scanning Confocal microscope (Nikon Instruments) equipped with a 60× oil objective. Images were subjected to deconvolution using Huygens

Professional (Scientific Volume Imaging). Colocalization coefficients (Rcoloc) of maximum intensity projection images were calculated using Nikon Elements (Nikon Instruments). Corrected total cellular fluorescence (CTCF) was measured using a previously described method (35). Briefly, area, integrated density and mean fluorescence were measured using ImageJ (v1.51q, NIH) for several cells, as well as for background signal. CTCF was calculated using the following equation: CTCF = integrated density − (area of selected cell × mean fluorescence of the background).

Biochemical analysis of tissues

Brain tissue from 3- to 4-month old parkin WT or knockout mice was dissected and homogenized in lysis buffer (10% w/v) containing 50 mM Tris–HCl pH 7.5, 150 mM NaCl, 1% Triton X-100, 5% glycerol, 1 mM EDTA and 1× Complete protease inhibitor cocktail (Roche) as previously described (36). Briefly, lysates were centrifuged at 100 000*g* for 30 min at 4°C and the soluble fraction was collected. Protein concentration was determined by BCA assay (Pierce Biotechnology) and equivalent levels of protein were resolved by SDS-PAGE followed by Western blot analysis with the desired antibodies. Ventral midbrain tissues from parkin $KO^{flox/flox}$ mice following intranigral injection of lenti-GFP-Cre or lenti-GFP were prepared in a similar manner (22,23).

Stereotactic surgery

Stereotactic injections were performed as previously described (37). Briefly, 3–4-month-old parkin WT or knockout mice received unilateral injections into the right substantia nigra (38) using the following coordinates relative to bregma: anterior–posterior, −2.9 mm; medio-lateral, −1.3 mm; dorso-ventral, −4.2 mm. Each mouse received ∼2.6×10^9 viral genomes (vg) of AAV2/6-VPS35-D620N or AAV2/6-MCS vector in a volume of 2 μl at a flow rate of 0.2 μl/min. Animals were sacrificed 12 weeks post-injection. Homozygous parkin cKO mice (floxed exon 7) at 6–8 weeks old received a single unilateral intranigral injection of lentiviral vector expressing GFP-Cre (or lenti-GFP as a control) and at 4 weeks post-injection ventral midbrain tissue was dissected for further analysis, as previously described (22,23).

Immunohistochemistry and stereological quantitation of neurons

Mice were anesthetized using tibromoethanol (avertin) and perfused-fixed with 4% PFA in 0.1 M phosphate buffer (pH 7.3). Brains were cryoprotected in 30% sucrose for 24 h before being sectioned using a microtome (Leica). Immunohistochemistry was conducted as previously described (39). Unbiased stereological methodology was used to estimate the number of substantia nigra dopaminergic neurons using the optical fractionator probe of the StereoInvestigator software (MBF Biosciences) as previously described (39). Briefly, every fourth coronal section (35 μm-thick) of the substantia nigra was immunostained with rabbit anti-TH antibody and counterstained with cresyl violet. All samples were blinded during stereological analyses.

Lentivirus and AAV production

Lentiviral vectors were prepared as previously described (26). Briefly, lentiviral vectors were produced in HEK-293T cells using a third generation packaging system, purified by centrifugation and resuspended in 1× PBS with 0.5% BSA. Viral titer was measured using the HIV-1 p24 antigen ELISA kit (Zeptometrix Corp). A p24 of 25 ng/ml was used to infect rat primary cortical neurons plated at a density of 500 000 cells in 3 ml of media in 35 mm dishes. Recombinant AAV2/6 viral vectors were produced and titered as previously described (24) by the University of North Carolina's Viral Vector Core. Viruses were diluted to a final concentration of ∼1.3×10^{12} vg per ml.

Supplementary Material

Supplementary Material is available at *HMG* online.

Acknowledgements

The authors thank Drs. Ted and Valina Dawson (Johns Hopkins University School of Medicine) for providing brain tissue from conditional parkin knockout mice. We thank Dr. Corinne Esquibel of the VARI Confocal Microscopy and Quantitative Imaging Core Facility for assistance with confocal microscopy and image processing/quantitation.

Conflict of Interest statement. None declared.

Funding

This work was supported by funding from Van Andel Research Institute (D.J.M.), Van Andel Institute Graduate School (E.T.W.), EPFL (D.J.M.) and the National Institutes of Health (R01 70NS105432 to D.J.M.).

References

1. Lang, A.E. and Lozano, A.M. (1998) Parkinson's disease. Second of two parts. *N. Engl. J. Med.*, **339**, 1130–1143.
2. Lang, A.E. and Lozano, A.M. (1998) Parkinson's disease. First of two parts. *N. Engl. J. Med.*, **339**, 1044–1053.
3. Hernandez, D.G., Reed, X. and Singleton, A.B. (2016) Genetics in Parkinson disease: Mendelian versus non-Mendelian inheritance. *J. Neurochem.*, **139 (Suppl. 1)**, 59–74.
4. Kitada, T., Asakawa, S., Hattori, N., Matsumine, H., Yamamura, Y., Minoshima, S., Yokochi, M., Mizuno, Y. and Shimizu, N. (1998) Mutations in the parkin gene cause autosomal recessive juvenile parkinsonism. *Nature*, **392**, 605–608.
5. Vilariño-Güell, C., Wider, C., Ross, O.A., Dachsel, J.C., Kachergus, J.M., Lincoln, S.J., Soto-Ortolaza, A.I., Cobb, S.A., Wilhoite, G.J., Bacon, J.A. *et al.* (2011) VPS35 mutations in Parkinson disease. *Am. J. Hum. Genet.*, **89**, 162–167.
6. Zimprich, A., Benet-Pagès, A., Struhal, W., Graf, E., Eck, S.H., Offman, M.N., Haubenberger, D., Spielberger, S., Schulte, E.C., Lichtner, P. *et al.* (2011) A mutation in VPS35, encoding a subunit of the retromer complex, causes late-onset Parkinson disease. *Am. J. Hum. Genet.*, **89**, 168–175.
7. Dawson, T.M. and Dawson, V.L. (2010) The role of parkin in familial and sporadic Parkinson's disease. *Mov. Disord.*, **25 (Suppl. 1)**, S32–S39.
8. Winklhofer, K.F. and Haass, C. (2010) Mitochondrial dysfunction in Parkinson's disease. *Biochim. Biophys. Acta*, **1802**, 29–44.
9. Malik, B.R., Godena, V.K. and Whitworth, A.J. (2015) VPS35 pathogenic mutations confer no dominant toxicity but partial loss of function in Drosophila and genetically interact with parkin. *Hum. Mol. Genet.*, **24**, 6106–6117.

10. Song, P., Trajkovic, K., Tsunemi, T. and Krainc, D. (2016) Parkin modulates endosomal organization and function of the endo-lysosomal pathway. *J. Neurosci.*, **36**, 2425–2437.
11. Braschi, E., Goyon, V., Zunino, R., Mohanty, A., Xu, L. and McBride, H.M., (2010) Vps35 mediates vesicle transport between the mitochondria and peroxisomes. *Curr. Biol.*, **20**, 1310–1315.
12. McLelland, G.L., Soubannier, V., Chen, C.X., McBride, H.M. and Fon, E.A. (2014) Parkin and PINK1 function in a vesicular trafficking pathway regulating mitochondrial quality control. *EMBO J.*, **33**, 282–295.
13. Narendra, D., Walker, J.E. and Youle, R. (2012) Mitochondrial quality control mediated by PINK1 and Parkin: links to parkinsonism. *Cold Spring Harb. Perspect. Biol.*, **4**, a011338.
14. Truban, D., Hou, X., Caulfield, T.R., Fiesel, F.C. and Springer, W. (2017) PINK1, parkin, and mitochondrial quality control: what can we learn about parkinson's disease pathobiology? *J. Parkinson's Dis.*, **7**, 13–29.
15. Pickrell, A.M. and Youle, R.J. (2015) The roles of PINK1, parkin, and mitochondrial fidelity in Parkinson's disease. *Neuron*, **85**, 257–273.
16. Kaiser, P. and Huang, L. (2005) Global approaches to understanding ubiquitination. *Genome Biol.*, **6**, 233.
17. Hierro, A., Rojas, A.L., Rojas, R., Murthy, N., Effantin, G., Kajava, A.V., Steven, A.C., Bonifacino, J.S. and Hurley, J.H. (2007) Functional architecture of the retromer cargo-recognition complex. *Nature*, **449**, 1063–1067.
18. Seaman, M.N. (2012) The retromer complex—endosomal protein recycling and beyond. *J. Cell Sci.*, **125**, 4693–4702.
19. Seaman, M.N., Gautreau, A. and Billadeau, D.D. (2013) Retromer-mediated endosomal protein sorting: all WASHed up! *Trends Cell Biol.*, **23**, 522–528.
20. McGough, I.J., Steinberg, F., Jia, D., Barbuti, P.A., McMillan, K.J., Heesom, K.J., Whone, A.L., Caldwell, M.A., Billadeau, D.D., Rosen, M.K. *et al.* (2014) Retromer binding to FAM21 and the WASH complex is perturbed by the Parkinson disease-linked VPS35(D620N) mutation. *Curr. Biol.*, **24**, 1678.
21. Zavodszky, E., Seaman, M.N., Moreau, K., Jimenez-Sanchez, M., Breusegem, S.Y., Harbour, M.E. and Rubinsztein, D.C. (2014) Mutation in VPS35 associated with Parkinson's disease impairs WASH complex association and inhibits autophagy. *Nat. Commun.*, **5**, 3828.
22. Shin, J.H., Ko, H.S., Kang, H., Lee, Y., Lee, Y.I., Pletinkova, O., Troconso, J.C., Dawson, V.L. and Dawson, T.M. (2011) PARIS (ZNF746) repression of PGC-1alpha contributes to neurodegeneration in Parkinson's disease. *Cell*, **144**, 689–702.
23. Stevens, D.A., Lee, Y., Kang, H.C., Lee, B.D., Lee, Y.I., Bower, A., Jiang, H., Kang, S.U., Andrabi, S.A., Dawson, V.L. *et al.* (2015) Parkin loss leads to PARIS-dependent declines in mitochondrial mass and respiration. *Proc. Natl. Acad. Sci. USA.*, **112**, 11696–11701.
24. Tsika, E., Glauser, L., Moser, R., Fiser, A., Daniel, G., Sheerin, U.M., Lees, A., Troncoso, J.C., Lewis, P.A., Bandopadhyay, R. *et al.* (2014) Parkinson's disease-linked mutations in VPS35 induce dopaminergic neurodegeneration. *Hum. Mol. Genet.*, **23**, 4621–4638.
25. Martinez, A., Lectez, B., Ramirez, J., Popp, O., Sutherland, J.D., Urbe, S., Dittmar, G., Clague, M.J. and Mayor, U. (2017) Quantitative proteomic analysis of Parkin substrates in Drosophila neurons. *Mol. Neurodegeneration*, **12**, 29.
26. Stafa, K., Trancikova, A., Webber, P.J., Glauser, L., West, A.B. and Moore, D.J. (2012) GTPase activity and neuronal toxicity of Parkinson's disease-associated LRRK2 is regulated by ArfGAP1. *PLoS Genet.*, **8**, e1002526.
27. Goldberg, M.S., Fleming, S.M., Palacino, J.J., Cepeda, C., Lam, H.A., Bhatnagar, A., Meloni, E.G., Wu, N., Ackerson, L.C., Klapstein, G.J. *et al.* (2003) Parkin-deficient mice exhibit nigrostriatal deficits but not loss of dopaminergic neurons. *J. Biol. Chem.*, **278**, 43628–43635.
28. Scott, K.L., Kabbarah, O., Liang, M.C., Ivanova, E., Anagnostou, V., Wu, J., Dhakal, S., Wu, M., Chen, S., Feinberg, T. *et al.* (2009) GOLPH3 modulates mTOR signalling and rapamycin sensitivity in cancer. *Nature*, **459**, 1085–1090.
29. Choudhury, A., Dominguez, M., Puri, V., Sharma, D.K., Narita, K., Wheatley, C.L., Marks, D.L. and Pagano, R.E. (2002) Rab proteins mediate Golgi transport of caveola-internalized glycosphingolipids and correct lipid trafficking in Niemann-Pick C cells. *J. Clin. Invest.*, **109**, 1541–1550.
30. Vonderheit, A. and Helenius, A. (2005) Rab7 associates with early endosomes to mediate sorting and transport of Semliki forest virus to late endosomes. *PLoS Biol.*, **3**, e233.
31. Sarbassov, D.D., Guertin, D.A., Ali, S.M. and Sabatini, D.M. (2005) Phosphorylation and regulation of Akt/PKB by the rictor-mTOR complex. *Science*, **307**, 1098–1101.
32. Moore, D.J., West, A.B., Dikeman, D.A., Dawson, V.L. and Dawson, T.M. (2008) Parkin mediates the degradation-independent ubiquitination of Hsp70. *J. Neurochem.*, **105**, 1806–1819.
33. Glauser, L., Sonnay, S., Stafa, K. and Moore, D.J. (2011) Parkin promotes the ubiquitination and degradation of the mitochondrial fusion factor mitofusin 1. *J. Neurochem.*, **118**, 636–645.
34. Beausoleil, S.A., Villen, J., Gerber, S.A., Rush, J. and Gygi, S.P. (2006) A probability-based approach for high-throughput protein phosphorylation analysis and site localization. *Nat. Biotechnol.*, **24**, 1285–1292.
35. McCloy, R.A., Rogers, S., Caldon, C.E., Lorca, T., Castro, A. and Burgess, A. (2014) Partial inhibition of Cdk1 in G 2 phase overrides the SAC and decouples mitotic events. *Cell Cycle*, **13**, 1400–1412.
36. Daniel, G., Musso, A., Tsika, E., Fiser, A., Glauser, L., Pletnikova, O., Schneider, B.L. and Moore, D.J. (2015) Alpha-Synuclein-induced dopaminergic neurodegeneration in a rat model of Parkinson's disease occurs independent of ATP13A2 (PARK9). *Neurobiol. Dis.*, **73**, 229–243.
37. Low, K., Aebischer, P. and Schneider, B.L. (2013) Direct and retrograde transduction of nigral neurons with AAV6, 8, and 9 and intraneuronal persistence of viral particles. *Hum. Gene Ther.*, **24**, 613–629.
38. Franklin, K.B.J. and Paxinos, G. (2008) *The Mouse Brain in Stereotaxic Coordinates, Compact*. Academic Press, Amsterdam, London.
39. Ramonet, D., Daher, J.P., Lin, B.M., Stafa, K., Kim, J., Banerjee, R., Westerlund, M., Pletnikova, O., Glauser, L., Yang, L. *et al.* (2011) Dopaminergic neuronal loss, reduced neurite complexity and autophagic abnormalities in transgenic mice expressing G2019S mutant LRRK2. *PLoS One*, **6**, e18568.